CHAPTER 2

Design and Synthesis of Large Arched Porphyrin-Spacer-Porphyrins (PSPs)

2.1 GEOMETRIC SURVEY AND COMPUTATIONAL ANALYSIS OF SPACER GROUPS

A directed synthetic approach toward the production of functionally active PSPs required particular attention to molecular design based on computational modelling of the various building blocks and of the overall PSP structure. This aspect of the project was especially important due to the significant effort involved in using a step-wise synthetic approach. A good understanding of the size, shape and final structural and functional details of a target PSP is necessary before any attempts at synthesis in order to increase the chances of successfully producing an active electron-transfer or catalytic system. Details of an early computational modelling survey of potential spacer groups and of the synthetic strategy adopted based on these results are presented in this chapter. A description of the subsequent synthesis of two different PSP systems based on the use of two analogous porphyrin blocks that incorporate various design elements based on the molecular models is also presented.

The key geometric features that were to be incorporated into the designed spacer groups of the target molecules required an efficient synthetic method. These systems also needed to be relatively rigid and suitably shaped for the precise positioning of the various components, including the two porphyrins and a centralised functional group. The simplest of the Basic Geometric Units (BGUs), outlined in Chapter 1 are the ribbon-like n-ladderanes.

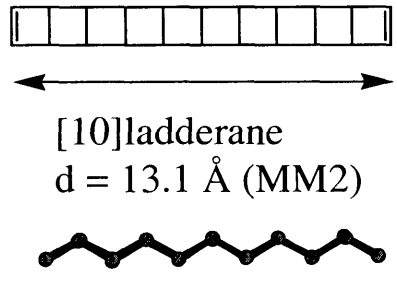

Figure 2.1 Structure and size of a typical ladderane showing a linear 'rod-like' geometry.

The ladderanes have a linear geometry and can be considered as molecular rods.[1] There is essentially no change in the linear shape of these systems with spacer length and the only real consideration in the structural analysis of them, therefore, is the distance between the two ends of the molecule as shown in Figure 2.1. In order to be used in the construction of a cofacial PSP, n-ladderanes would have to be connected to 'angle' blocks at each end as well as to a central functionalised block. The reported study on a variety of 'chevron-shaped' centrosymmetric ladderane structures, containing a central norbornane unit (homo[n]ladderanes), provides an example of how ladderane-type sub-units could be incorporated into larger spacer groups.[1,2] Warrener and co-workers used computed molecular mechanics models to demonstrate that geometrical control of the apical angle of the central norbornyl-type unit, through variation of the central bridge atom type, was possible.[2] The calculated angles and distances from that study are summarised in Table 2.1.

Table 2.1 Effect of bridge atom type (R) on angle ABC and on terminal-terminal distance (d) on a chevron-shaped centrosymmetric ladderane structure.[2]

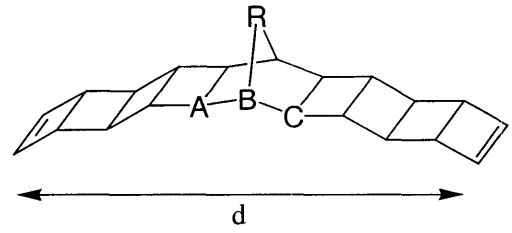

R	Angle ABC (deg.)	d (Angstroms)
O	110.6	12.94
C=O	107.8	12.97
$C{=}CH_2$	107.9	12.97
NH	108.7	12.94
S	106.8	12.94
CH_2	106.1	12.88
cyclopropyl	104.7	12.88
$C(CH_2)_2$	99.9	12.49

A significant effect on the apical angle is seen upon replacement of a methylene bridge with an oxygen bridge resulting in a 'flatter' or less bent shape. This result is also relevant in the consideration of polynorbornyl structures.

The curved nσ-binanes and [n]polynorbornanes, introduced in Chapter 1 (Figure 1.26), vary in inter-terminal distance as well as in shape (i.e. curvature) depending on the backbone of the molecule and the stereochemistry of the fused sub-units. However, due to the multiplicity of synthetic steps and the low overall yields expected for large functionalised systems, the use of a ladderane framework was dismissed as a strategy for the synthesis of PSPs in the present study. Nevertheless, the ruthenium catalysed [2+2] cycloadditions used in building up the ladderane structures have also been shown to be useful in extending other spacer systems and could be used in the design of our molecules. A number of prototypical nσ-binanes and [n]polynorbornanes were modelled in order to find systems that could be used for generating PSPs and these are shown in Figures 2.2, 2.3, 2.5 and 2.6. The Molecular Mechanics (MM2) level of calculation was used and found to be adequate for this initial survey as an overall general picture was being sought. The use of higher levels of theory at this stage was not practical considering the size of the systems being examined. Nevertheless some general trends in size and shape can be seen from the series of structures presented.

To form a catalytic PSP capable of binding several organic molecules simultaneously, a reasonably large open cavity is required, so it follows that a relatively large spacer group is also necessary. An early idea was to use either a binane or polynorbornane type spacer that had an acutely angled or 'bent' attachment point at each end. The terminal bent groups could be formed, in principle, by tandem [2+2] cycloadditions between a *bis*-cyclobutene diester precursor and cyclopentadiene as outlined in Chapter 1 (Section 1.4.2). Thus a regular series of potential spacer groups were modelled (Figures 2.2 and 2.3). In the first series (Series A in Figure 2.2), fixed end-groups were maintained in a basic σ = 8 unit while the number of intervening *bis-exo,exo*-fused cyclobutane norbornyl (σ = 4) bridge units* were varied. In a second series (Series B in Figure 2.3), the same fixed end-groups were maintained while the number of intervening norbornyl (σ = 2) bridge units were varied. Analogous oxa-norbornyl systems were also modelled in both series.

---

* Extension is by successive fusion with a tetracyclo[6.2.1.$0^{2,7}0^{3,6}$]decane-3,6-dicarboxylic acid dimethyl ester unit or its oxa-bridged analogue

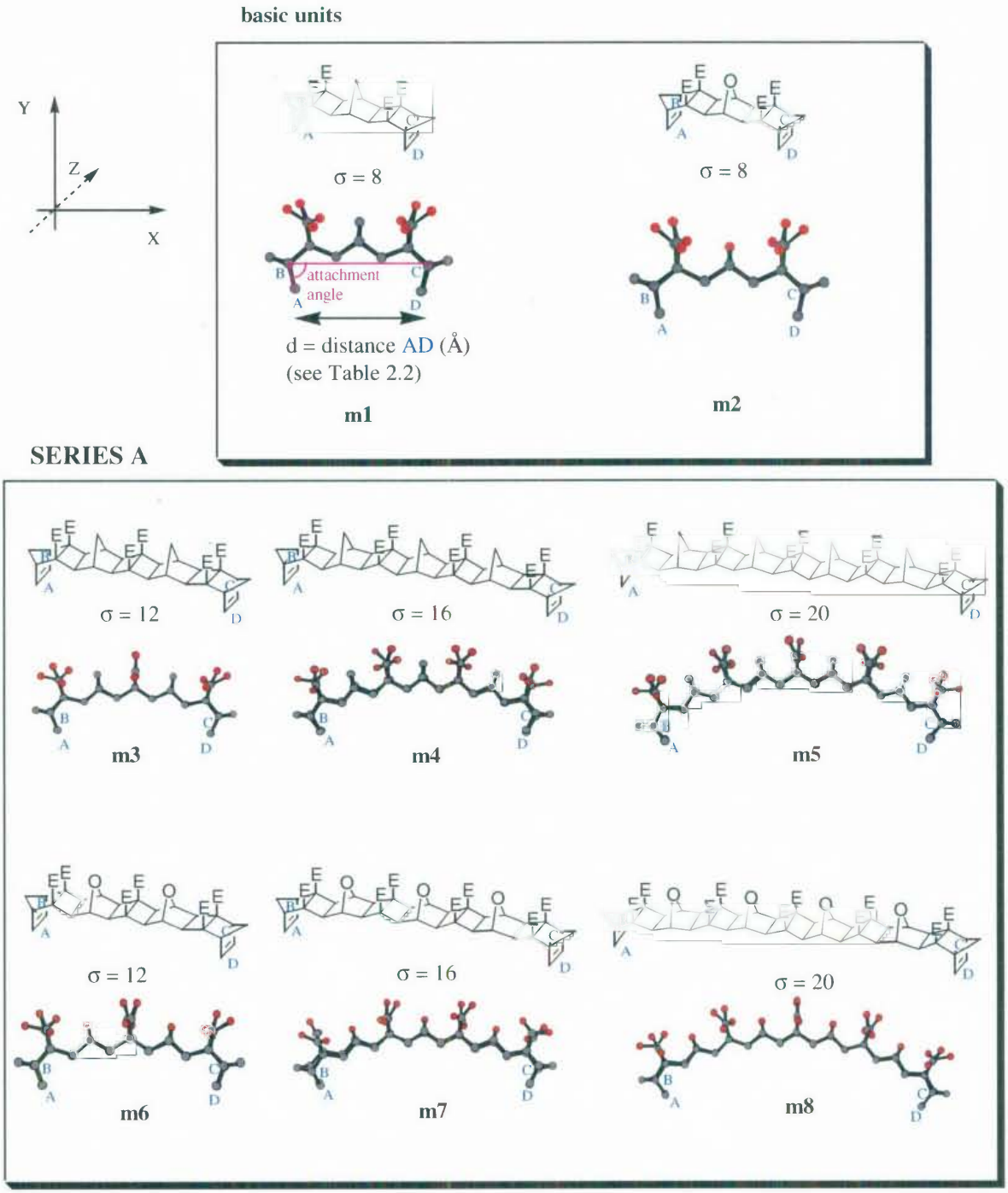

Figure 2.2 Geometric survey of potential spacer groups (acute): members of Series A ('bent' binanes) are extensions of model 1 (**m1**, methylene bridge) or **m2** (oxygen bridge). The 'attachment angle', ∟**ABC**, has been used for a general comparison between different spacer groups (Table 2.2). Points **B** and **C** are centroid positions along the Z-axis (into the page) between the penultimate carbon atoms at each end of the molecule and Points **A** and **D** are centroid positions along the Z-axis between the two terminal carbon atoms at one end of the molecule. The inter-terminal distance, **d**, is between points **A** and **D** (Table 2.2). σ defines the number of single bonds along the X-axis (Table 2.2).

References, p. 106

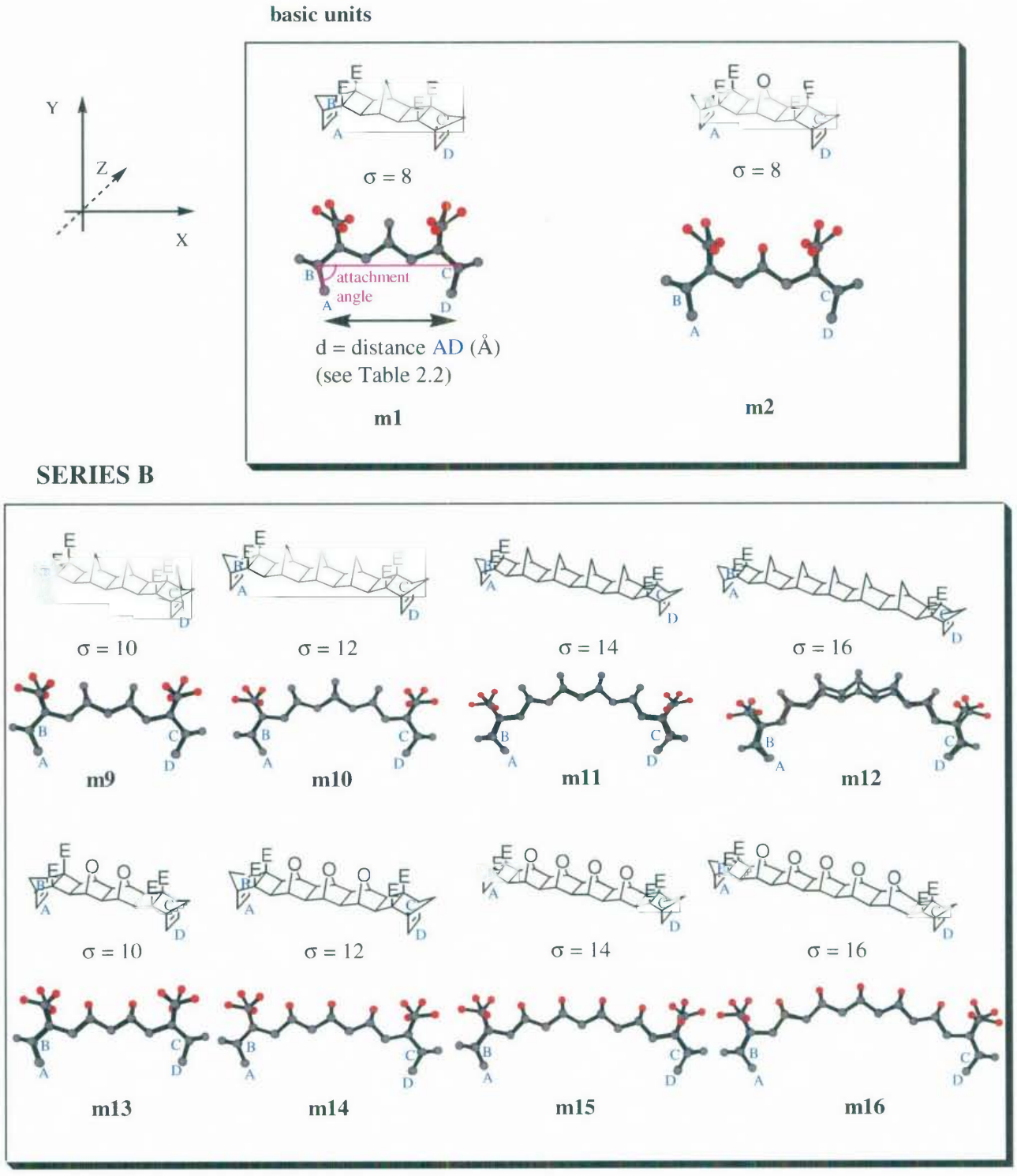

Figure 2.3 Geometric survey of potential spacer groups (acute): members of Series B ('bent' polynorbornanes) are extensions of model 1 (**m1**, methylene bridge) or **m2** (oxygen bridge). The 'attachment angle' (∟**ABC**); points **B, C** and **D**; inter-terminal distance, **d**; and σ are all defined as in Figure 2.2 and results are presented in Table 2.2.

The attachment angle (∟ABC) is defined (Figure 2.2) for easy comparison with an 'ideal' system (∟ = 90°) in which there would be a parallel cofacial *bis*-porphyrin arrangement if a linear attachment protocol were to be used. One significant trend in these systems is that an increase in inter-terminal distance, **d**, leads to an increase in curvature and a concomitant decrease in the attachment angle. The curvature of the 'bent' polynorbonanes (Series B in Figure 2.3) is more pronounced than in the 'bent' binanes (Series A in Figure 2.2). The calculated values of **d** and the respective attachment angles of all the models presented in Figures 2.2 (**m1-m8**) and 2.3 (**m9-m16**) are given in Table 2.2. A slight increase in both the attachment angle and **d** upon replacing the carbon bridging-atoms (**m3-m5**) with oxygen bridging-atoms (**m6** to **m8**) was predicted for the 'bent' binanes (Series A) whereas a more pronounced effect was calculated for the 'bent' polynorbornanes (Series B) where both the attachment angles and **d** values are significantly larger in the oxa-bridged systems (**m13-m16**) compared with the analogous methylene bridged systems (**m9-m12**) (Figure 2.3 and Table 2.2).

Table 2.2 Calculated (MM2) inter-terminal distance (**d**) and attachment angle (∟**ABC**) for each of the 'bent' binane-type (Series A: **m1-m8** in Figure 2.2) and 'bent' polynorbornyl-type (Series B: **m9 – m16** in Figure 2.3) spacer groups

Model (Fig. 2.1)			σ	d (Å)	∟ABC
m1 (CH_2)			8	6.9	75.5
m2 (O)			8	7.1	77.8
Series A	**CH_2**	**m3**	12	11.3	66.2
		m4	16	15.5	58.7
		m5	20	19.7	52.4
	O	**m6**	12	11.5	68.8
		m7	16	15.9	62.7
		m8	20	19.8	54.1
Series B	**CH_2**	**m9**	10	8.7	66.6
		m10	12	10.3	57.0
		m11	14	11.7	49.8
		m12	16	13.4	44.7
	O	**m13**	10	9.2	72.6
		m14	12	11.2	66.8
		m15	14	13.3	62.9
		m16	16	14.6	53.6

These calculations indicate that the resulting 'bent' binane and 'bent' polynorbornane structures must be ruled out because two attached porphyrin groups would be either juxtaposed or in very close contact, largely as a result of the acute attachment angles (∟ABC), and would therefore lead to a small closed cavity if it could be formed at all. To illustrate this point molecular modelling (MM2) of a porphyrin ring variously attached to the 'bent' binane spacer group (**m1**) was carried out and the resulting structures are presented in Figure 2.4. Three different attachment protocols were modelled; direct attachment, attachment using a pyrazine linker and attachment through a pyrazino[2,3-*g*]quinoxaline linker. Both the pyrazine and pyrazino[2,3-*g*]quinoxaline linkers would be formed from the coupling of complementary α-diones and aromatic α,β-diamines. The length of the 'side arm' was a major consideration when using spacer groups with acute attachment angles (for any given acute attachment angle, the larger the side arm the closer the approach of the terminal porphyrin units). Clearly for all structures, attachment of a second porphyrin moeity at the opposite end of the spacer unit would be sterically impossible.

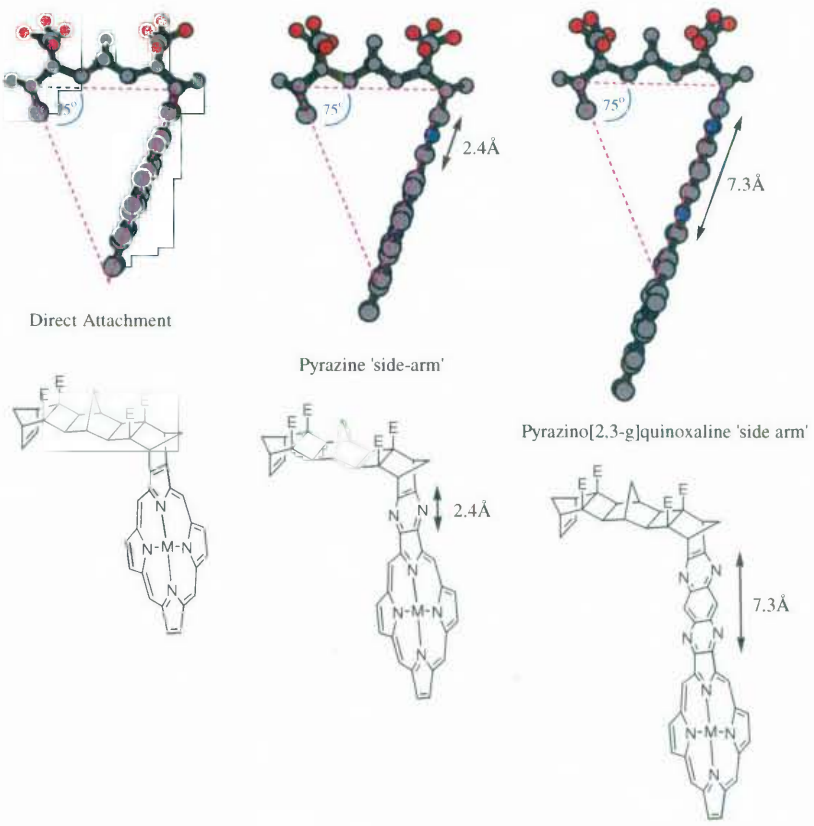

Figure 2.4 Comparison of different attachments of a porphyrin ring to a convergent 'bent' binane spacer (**m1**). Larger binane spacers in this series (e.g. **m3**-**m5**) have even smaller attachment angles.

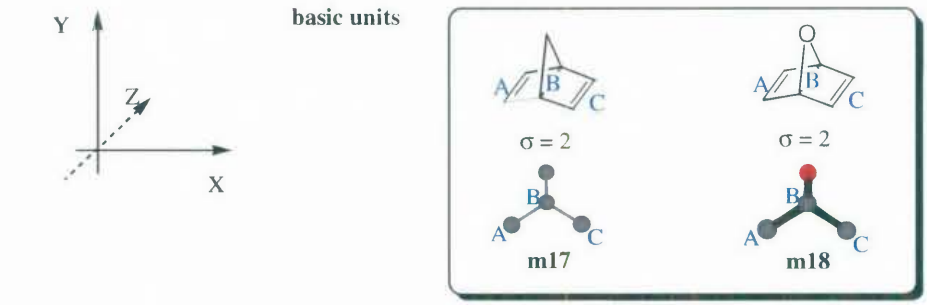

SERIES C

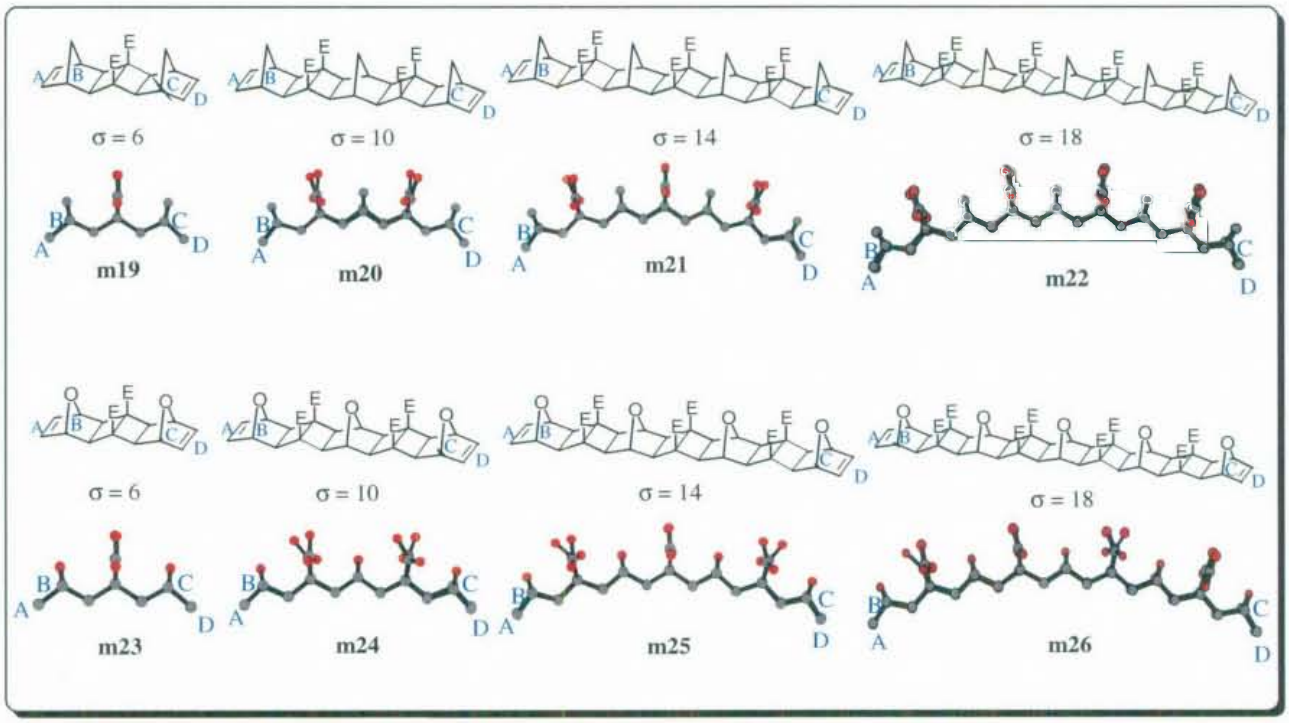

Figure 2.5 Geometric survey of potential spacer groups (obtuse): members of Series C (binanes) are all extensions of model 17 (**m17**, methylene bridge) or **m18** (oxygen bridge). The 'attachment' angle (∟**ABC**); points **A**, **B**, **C** and **D**; the inter-terminal distance, **d**; and **σ**, are all defined as in Figure 2.2. The calculated values of the attachment angles and inter-terminal distances, **d**, are presented in Table 2.3.

Direct attachment to a binane or polynorbornane spacer, without the 'bent' terminal groups, was also considered. A selection of alternative representative structures was modelled and these are shown in Figures 2.5 (Series C: binanes) and 2.6 (Series D: polynorbornanes). The backbones of these systems are identical to the analogous 'bent' analogues already discussed and the increasing curvature with size is also a feature.

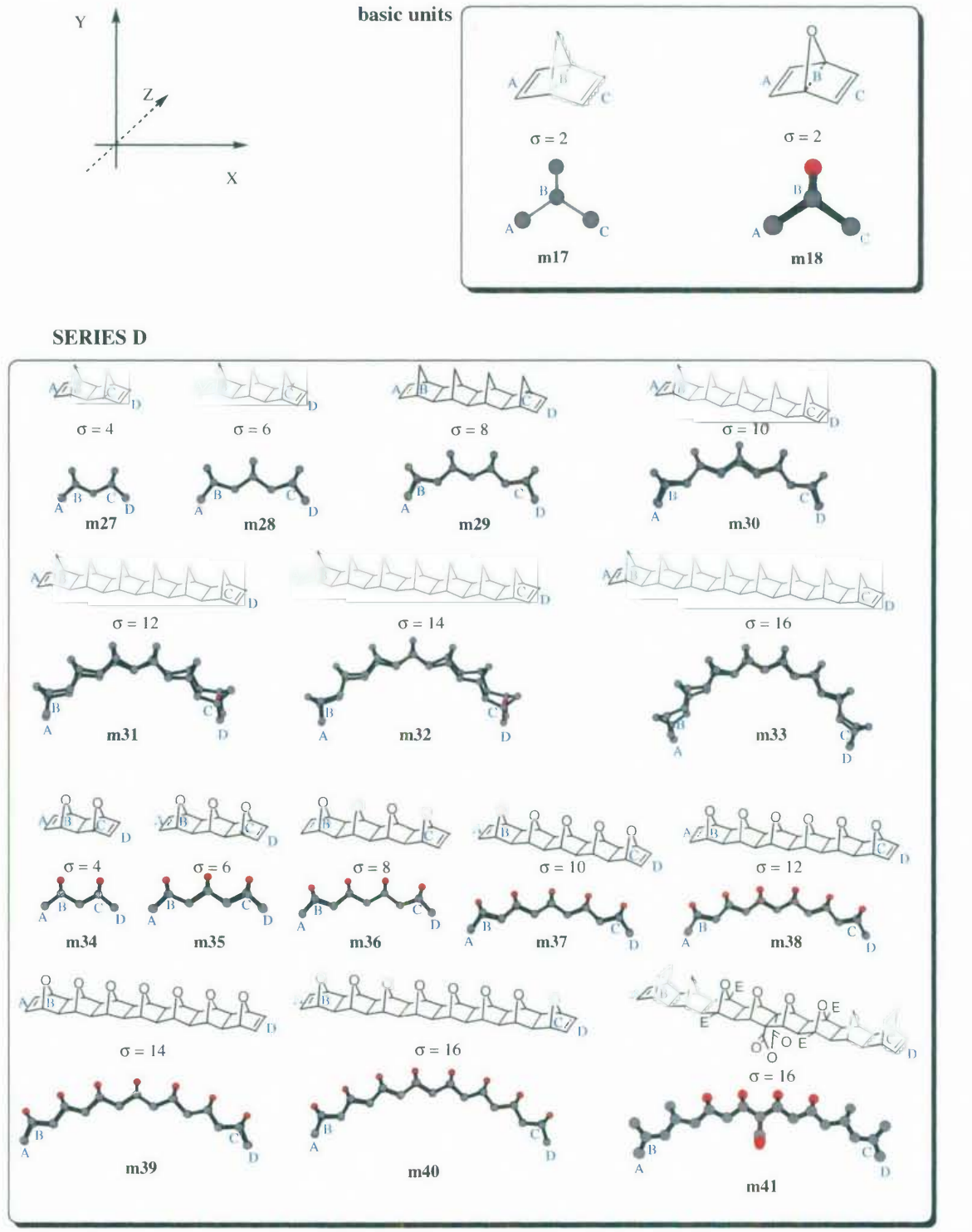

Figure 2.6 Geometric survey of potential spacer groups (obtuse): members of Series D (polynorbornanes) are all extensions of model 17 (**m17**, methylene bridge) or **m18** (oxygen bridge). The 'attachment' angle (∟**ABC**); points **A**, **B**, **C** and **D**; the inter-terminal distance, **d**; and σ, are all defined as in Figure 2.2. The calculated values of the attachment angles and inter-terminal distances, **d**, are presented in Table 2.3.

Table 2.3 Calculated (MM2) inter-terminal distance (**d**) and attachment angle (∟**ABC**) for each of the binane (Series C) and polynorbornyl (Series D) spacer groups (**m17-m41** in Figures 2.5 and 2.6).

Model (Fig. 2.1)			σ	d (Å)	∟ABC
m17 (CH_2)			2	2.4	112.9
m18 (O)			2	2.4	110.5
Series C	**CH_2**	**m19**	6	7.5	138.2
		m20	10	12.2	127.6
		m21	14	17.0	121.3
		m22	18	21.9	118.3
	O	**m23**	6	7.5	138.2
		m24	10	12.4	133.1
		m25	14	17.0	121.5
		m26	18	21.9	118.3
Series D	**CH_2**	**m27**	4	4.8	136.8
		m28	6	7.1	126.7
		m29	8	9.2	116.5
		m30	10	11.1	108.6
		m31*	12	12.6	97.3
		m32*	14	14.0	88.7
		m33*	16	14.4	80.4
	O	**m34**	4	4.9	139.9
		m35	6	7.3	135.6
		m36	8	9.7	130.3
		m37	10	12.0	125.0
		m38	12	14.2	119.5
		m39	14	16.1	112.9
		m40	16	18.0	107.8
	block	**m41**	16	18.5	112.0

* **m31-m33** exhibited various degrees of twisting.

The binanes, in general, are less curved than the polynorbornanes and, therefore, are less suitable as spacer groups if a direct or linear attachment protocol were to be used, as widely *divergent* PSP systems would be formed. A comparison of the two σ = 10 systems (**m20** and **m30**) demonstrates this clearly (Table 2.3). The obtuse polynorbornane attachment angle (109°) of **m30** is about twenty degrees less than the binane (**m20**) attachment angle (128°). Attachment angles for the larger polynorbornane spacers are approaching the 'ideal' situation and so, geometrically speaking, they became interesting potential candidates. The calculated values of **d** and the respective attachment angles of all the models presented in Figures 2.5 (**m17-m26**) and 2.6 (**m27-m40**) are given in Table 2.3.

The incorporation of a centralised functional group was then considered. One group of compounds that had already been used successfully for making cofacial crown ether systems was the fused *bis*-oxanorbornene imides (**4**) (Scheme 2.1 p70).[3,4] The chemistry needed to extend these imides to the corresponding cyclobutene diesters (**5**) and cyclobutane epoxides (**6**) and further coupling to a norbornyl unit via a building block approach had already been established as discussed in Chapter 1 (Section 1.4.2).[5] The method for the production of a hetero-polynorbornyl spacer group (**8**), with the required central functionality was, therefore, feasible. The analysis of such a structure using molecular modelling (**m41** in Figure 2.6) showed it to have the characteristic curved shape of the polynorbornyl spacer groups (Series D in Figure 2.6) as well as having an attachment angle of around 112°, which would lead to a system where the two porphyrin units were somewhat divergent. It was decided that a critical angle of divergence was not a serious impediment to the production of active PSP electron-transfer and/or catalytic systems.

The effect of porphyrin unit divergence on the activity of the electron-transfer device, based on the design principles outlined in Chapter 1 (Figure 1.33), would be related to comparatively larger inter-porphyrin distances compared to an analogous parallel PSP. The covalently attached electron acceptor unit (armature) in the designed electron-transfer device would have to traverse a larger distance (**d1** in Figure 2.7) and so it would be expected that the forward electron-transfer process might be less efficient, however, the reverse recombination process would also be retarded and the balance of these would have to be determined experimentally. In the long term other PSPs of different shape and size would be needed for comparison. The larger inter-porphyrin distance (**d2** in Figure 2.7) in a divergent PSP artificial enzyme, based on the design principles outlined in Chapter 1 (Figure 1.34), is, in itself, not expected to be a problem as larger complementary

substrates can be used. Possibly more important is the change in bonding angle between the porphyrin metal centre and the substrate(s) and the effect of this on the orientation of the substrates before and during a reaction between them. Molecular modelling suggests that two substrate molecules bound orthogonally to the inside of each porphyrin-unit will still be oriented toward one another although the point of contact between them will be relatively 'lower' in the cavity compared with a parallel *bis*-porphyrin. In a parallel system the substrates would be 'in line' with one another with an orientation of 180° whereas in a divergent *bis*-porphyrin based on **m41** (Figure 2.6) the substrates would be positioned with an orientation angle (Figure 2.7) of 136° to one another.*

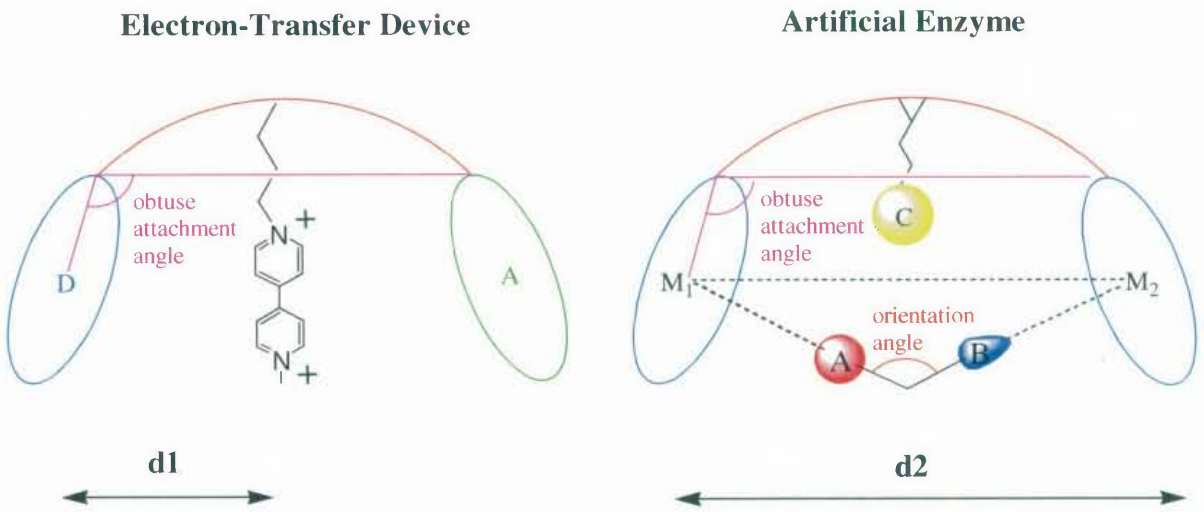

Figure 2.7 Schematic representation of the electron-transfer device and artificial enzyme designs based on obtuse attachment angles.

A slightly divergent (or convergent) PSP system is very likely to be more effective than a parallel system where the reaction being catalysed involves a transition state in which the substrate molecules are similarly oriented. Although predictions can be made based on molecular modelling it is necessary to test the capabilities of all such systems experimentally in order to gain insight into the importance of the various geometric factors.

---

* The 'orientation angle' (X) (see Figure 2.7) between two substrate molecules is related to the 'attachment angle' (Y) by the equation:
$X = 360° - 2Y = 360° - 224° = 136°$. Also see Figure 3.1 in the following chapter for a detailed geometric description of a PSP.

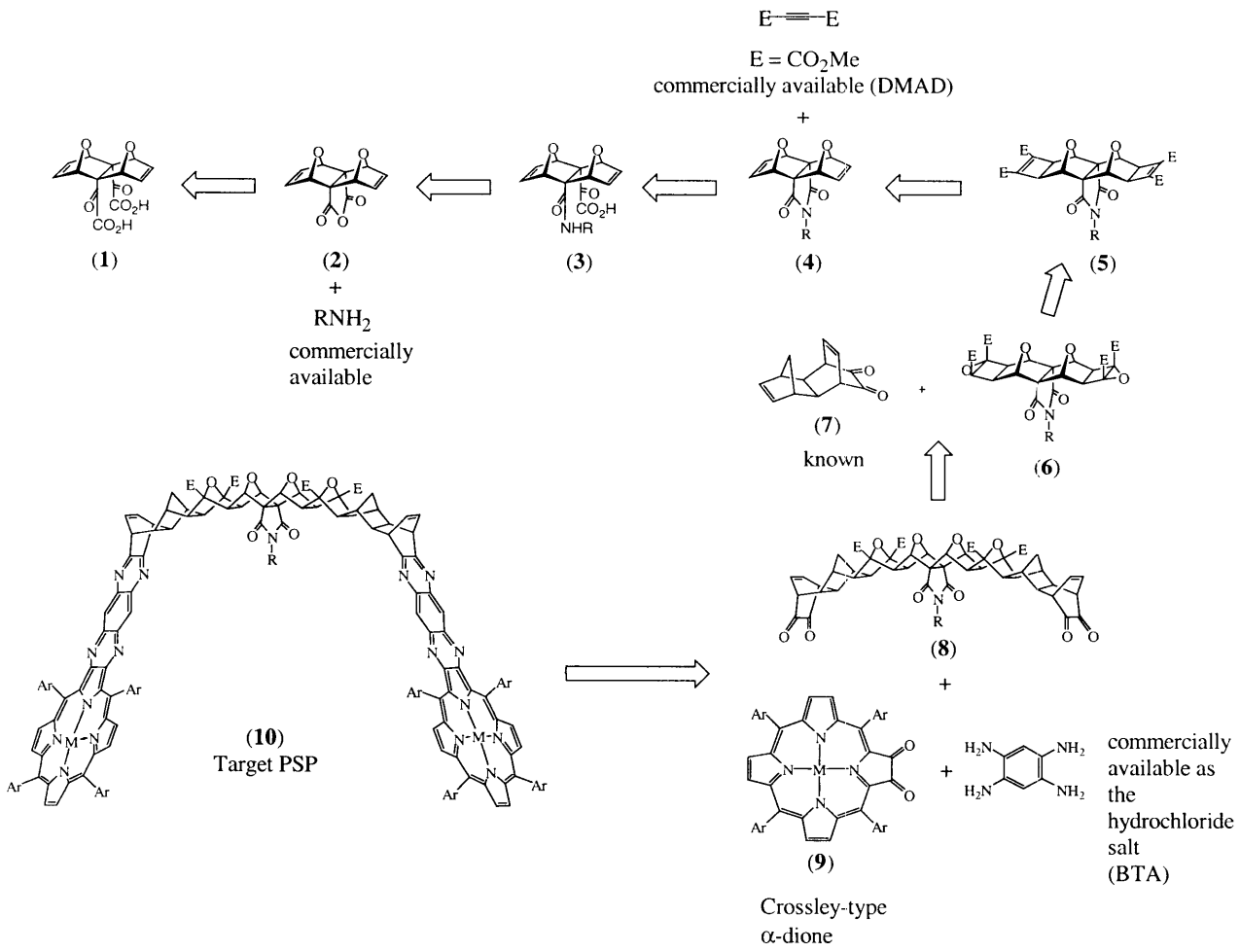

Scheme 2.1 Retrosynthetic analysis of the target PSP (**10**).

Given the results of these modelling studies of the geometries the spacer systems based on the fused oxa-bridged norbornenes were targeted. The synthesis of the spacer blocks with central functionality, porphyrin blocks (PBlocks) based on Crossley-type porphyrin α-diones (**9**) and the subsequent synthesis of PSPs based on these building blocks will be the main focus of the remainder of this chapter. The retrosynthetic analysis of the target PSP is outlined in Scheme 2.1. All the building blocks for the spacer group were based on known compounds and further development of these particular spacers relied on the efficient introduction of a centralised, 'downward-facing' functional unit onto the fused oxa-bridged norbornenes.

2.2 *EXO,EXO*-FUSED *BIS*-OXABRIDGED NORBORNENE IMIDES

2.2.1 FUNCTIONAL APPLICATIONS

There were a number of different roles that were envisaged for various imide functional groups depending on the stage of electron/energy transfer and artificial enzyme system development (Section 1.5). In the early stages of development a strategically placed functional group could act simply as an analytical tool in order to establish extra structural information about the PSP systems. An example of this is the positioning of a particular group so that its chemical environment could be altered upon binding of an aromatic substrate. Such a group has been classed in this work as a 'probe' and would find application in early NMR experiments designed to analyse the structure of the particular PSP. Other functional groups could be incorporated as additional binding sites (e.g. through hydrogen bonding) or as catalytic sites (e.g. through proton or electron transfer) hopefully adding to the catalytic activity in the final stages of artificial enzyme development. Introduction of a chiral group into this central position would be useful for increasing the selectivity of the system toward chirally active substrates. Finally, these imides offer a way of introducing a mobile electron-transfer unit, or 'armature', in a unique molecular switch design. A synthetic method based on the assembly of building blocks allows for an efficient development of these various systems once the initial synthetic protocols have been established. All that is required is the replacement of the central functional group during building block construction.

The synthesis of suitably functionalised *exo,exo*-fused *bis*-oxabridged norbornene imides seemed straightforward starting from the corresponding norbornene anhydride (**2**) (Scheme 2.1 and 2.2). The formation of alkyl imides from this compound had already been reported, as mentioned previously, so the way seemed clear to make a number of these derivatives with appropriately designed functionality.

2.2.2 ARYL IMIDES

In order to position functional groups precisely a rigid tether was required. One simple option was to use suitably functionalised aromatic amines. Aromatic systems of different size, shape and functionality offer structural and functional design flexibility. The first targets in this series were designed to position a group within the cavity to act as a structural probe. Molecular modelling

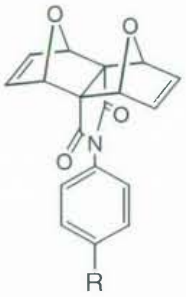

(**20**) R = *tert*-butyl
(**21**) R = OMe

(AM1) of a typical proposed PSP system (**m42** in Figure 2.8) showed that either a *tert*-butyl or methoxy group, in the 4' position of an aryl imide (**20**) and (**21**) could be useful as structural probe units. The methyl hydrogens of both probe groups were predicted to be as close as 3.7 Å to the inter-porphyrin plane. Binding of an aromatic substrate between the porphyrin sub-units, for instance, would be expected to affect the NMR chemical shift of these methyl protons giving information about the binding geometry and distances.

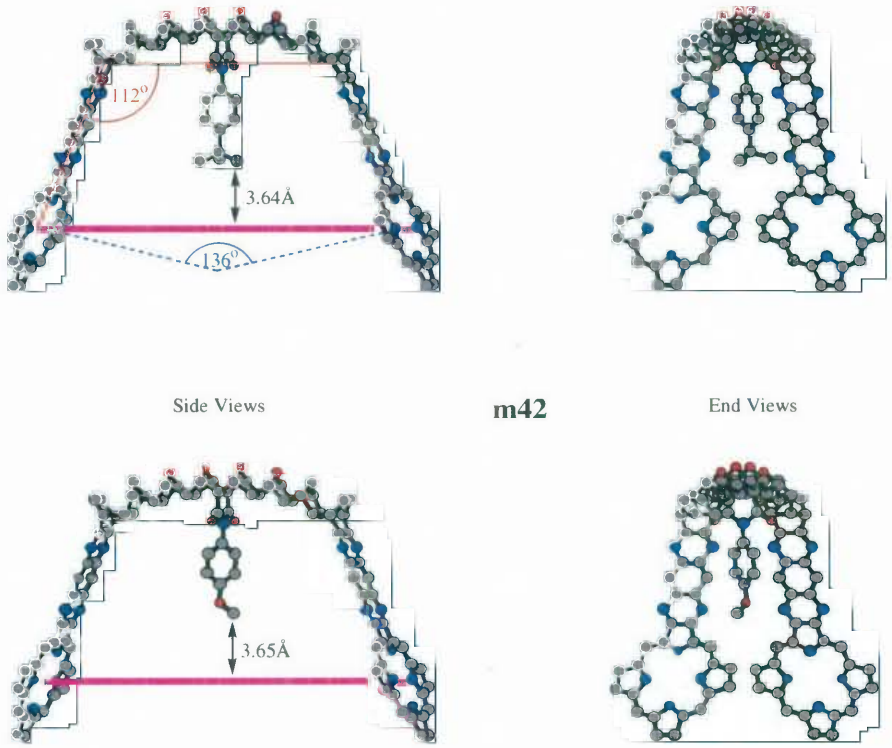

Figure 2.8 Molecular model (**m42**: AM1) of the skeletal structure of a proposed PSP system, with a methyl group (*tert*-butyl or methoxy) suitably positioned to act as an NMR structural probe. The methyl-hydrogen to interporphyrin-plane pink line) distance was calculated from the static molecular model. Larger average distances between the methyl hydrogens and the inter-porphyrin plane are predicted if free rotation of bonds is taken into account.

2.2.3 SYNTHESIS OF ANHYDRIDE (**2**)

It has been shown that the stereospecific Diels-Alder reaction between furan and acetylene dicarboxylic acid gives exclusively the *exo,exo-bis*-oxabridged norbornene dicarboxylic acid (**1**).[6] Subsequent ring closure using $SOCl_2$ gives the anhydride (**2**) (Scheme 2.2).[3,7] It is important to note that the *exo,exo*-adduct (**1**) is the kinetic product formed at room temperature and precipitates

from solution upon formation. It has been proposed that the formation of the *exo,exo*-adduct, in preference to more stable *exo,endo*- or *endo,endo*-adducts is solubility driven.[8] These reactions were repeated giving the dicarboxylic acid (**1**) in 50% yield and the anhydride (**2**) in 58% yield. The identity of the anhydride was confirmed by comparison with published ^{1}H and ^{13}C NMR spectral data and melting point.

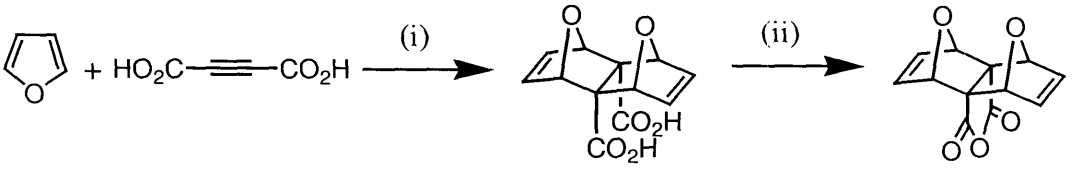

(**1**) 50% (**2**) 58%

Scheme 2.2 Synthesis of fused *bis*-oxabridged norbornene anhydride according to literature methods.[3,6] Reagents and Conditions: (i) r.t., diethyl ether, 2-3 weeks (ii) $SOCl_2$, Δ 80-85°C, N_2 atm, 2 hrs.

2.2.4 SYNTHESIS OF ARYL AMIC ACIDS AND IMIDES

2.2.4.1 Attempted Synthesis of an aryl amic acid (**13**): Conventional Methods

The general approach planned for the synthesis of targeted amic acids and imides represented by general formulae (**3**) and (**4**) makes use of a simple two-step reaction sequence (Scheme 2.3). The first step is the formation of an aryl amic acid from the reaction of (**2**) with a *para*-substituted aniline derivative. The usual method for the synthesis of alkyl amic acids involves heating an alkyl amine with the anhydride (**2**) over several days. Subsequent dehydration of the amic acid gives the respective imide. A common method used for the dehydration of alkyl amic acids involves heating with sodium acetate in acetic anhydride.[3]

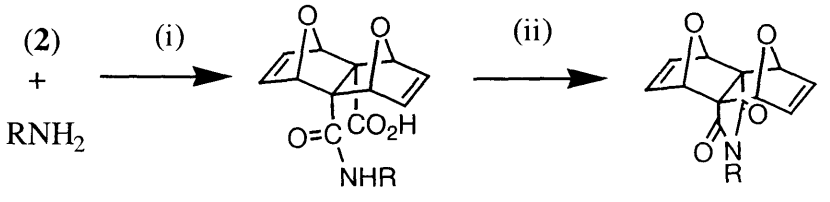

(**3**) (**4**)

Scheme 2.3 General synthesis of amic acids and imides from fused *bis*-oxabridged norbornene anhydride (**2**).[3] Reagents and Conditions: (i) heat (ii) $NaOAc/Ac_2O$, heat.

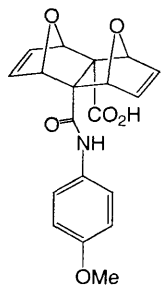

(13)

The reactivity of aniline derivatives with (**2**) was unknown and a number of different experimental conditions were tested. A refluxing equimolar solution of the anhydride (**2**) and anisidine in $CDCl_3$ was monitored over a period of 7 days by ^1H NMR spectroscopy. After 7 days the reaction mixture consisted almost entirely of starting materials. None of the expected reaction product (**13**) was detected under these conditions. The solvent was then removed and the neat reactant mixture was heated at 60°C for 1 day, but still no reaction had occurred. A further increase in temperature (100°C) again failed to induce the formation of the desired product (a number of small peaks in the aromatic region of the ^1H NMR spectrum may indicate oxidation of anisidine; it is known that aromatic amines are easily oxidised in the presence of oxygen). A repeat of these experiments using a five-fold excess of anisidine gave similar negative results.

2.2.4.2 Attempted Synthesis of Amic Acid (**13**): High Pressure Method

Due to the problems faced with forming the desired aryl amic acid (**13**) it was decided to try the same reaction under high-pressure conditions (7-14 kbar). This was rationalised as follows. Reversible reactions that involve a change in volume are affected by pressure according to equation (2). The volume of reaction, ΔV, corresponds to the difference between the partial molar volumes of reactants and products. Where ΔV is negative an increase in pressure will drive the equilibrium toward the side of the products and vice versa. A similar treatment using transition state theory predicts that any reaction with a negative activation volume, $\Delta V^{\ddagger}$, will be accelerated under high-pressure conditions according to equations (3) and (4).[9-11]

$$-RT\left(\frac{\partial}{\partial P}\ln K\right)_T = \frac{\partial \Delta G}{\partial P} = \Delta V \qquad (2)$$

where;

K = the thermodynamic equilibrium constant involving ground-state reactant(s) and product(s)

$$k_p = (k/h)K^{\ddagger} \qquad (3)$$

= the rate constant of a liquid phase reaction (at pressure, p)

where;

$K^{\ddagger}$ = the equilibrium constant for the formation of the transition state

h = Planck constant

k = Boltzmann constant

$$-RT\left(\frac{\partial}{\partial P}\ln k_p\right)_T = -RT\left(\frac{\partial}{\partial P}\ln K^{\ddagger}\right)_T = \left(\frac{\partial \Delta G^{\ddagger}}{\partial P}\right)_T = \Delta V^{\ddagger} \qquad (4)$$

For reactions in solution, the activation volume, $\Delta V^{\ddagger}$, can be treated as consisting of two terms; $\Delta V_1^{\ddagger}$, the changes in the volumes of the reactants themselves and $\Delta V_2^{\ddagger}$, the change in the volume of the surrounding solvent cage. Any reaction that starts with neutral reactants and involves the formation, or partial formation, of charge in the transition state will be accelerated with increasing pressure according to this theory. The overriding effect in these instances is the change in the volume of the solvent cage, $\Delta V_2^{\ddagger}$, and is caused by electrostriction of the nearby solvent cage around the developing charges. It follows that the largest effect will be noticed in non-polar solvents, and different workers in the field have demonstrated this experimentally. Perrin and Williams, who studied a series of S_N2 (Menschutkin) reactions, noticed these effects over six decades ago.[12] A recent example involving sequential S_N2 substitution reactions is the reported formation of a number of tetracationic catenanes and rotaxanes using pressures of up to 12 kbar. The same systems either could not be made, or were formed in extremely low yields at atmospheric pressure.[13,14]

A large number of reaction types have been studied by various workers and several recent reviews and books give a good account of both the theoretical and experimental aspects of high-pressure reactions.[15-18] In particular, a number of reaction types that involve the generation of ionic species have been reported to be accelerated by high-pressure conditions including: aliphatic and aromatic nucleophilic substitutions; addition of nucleophiles to electron deficient alkenes and oxiranes; and peptide formation from esters.[18] As shown in Figure 2.9 intermediates 1 and 2 in the addition-elimination mechanism describing the reaction between aniline derivatives and an anhydride such as (**2**) are both ionic and thus the dominant electrostriction of the surrounding solvent shell is expected to lead to a decrease in volume. The equilibrium should, therefore, be shifted forward under high-pressure conditions. Also the transition state theoretical treatment predicts that the formation of intermediate 1 will be accelerated by an increase in pressure. Overall it is expected from theory that the formation of both intermediates will be promoted under high-pressure conditions.

References, p. 106

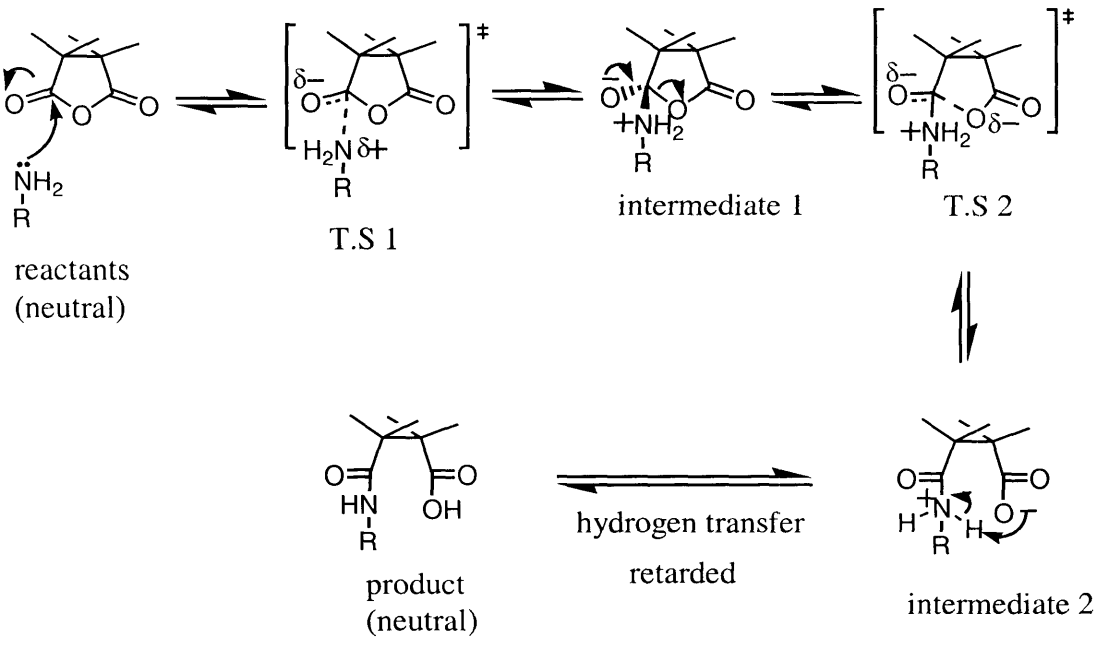

Figure 2.9 Addition and elimination transition states for the acetylation of a primary amine involving an anhydride. Partially charged transition states should be stabilised by high pressure through electrostriction-induced volume contraction of the solvent cage.

The anhydride (**2**) and anisidine were partially dissolved in a small volume of CH_2Cl_2 (4-5 mL) and placed under a pressure of 7 kbar for 24 hours. ^{1}H NMR spectral analysis of the reaction mixture showed that little change had occurred. A repeat of the experiment using higher pressures (13 kbar) over a longer period of time (2.5 days) led to the conversion of all starting materials into an uncharacterised product.

The expected amic acid was not present, according to the ^{1}H NMR spectrum of the crude product*; however, treatment of the crude product with NaOAc and Ac_2O at 60°C for 3 days did give the desired imide (**21**) in moderate yield (Scheme 2.4 and Table 2.4). As the imide (**21**) was obtained after dehydration, it is likely that the *bis*-amide was formed instead of the amic acid and the main peaks in the ^{1}H NMR spectrum of the crude reaction mixture are consistent with this hypothesis, however, the intermediate was neither isolated nor characterised. Despite the ambiguity surrounding the identity of this intermediate, the use of high-pressure conditions was demonstrated to be a valid method towards the production of the desired aryl imide in moderate yield where a reaction using standard conditions failed. This success offered an entry point to the

* It was initially assumed that the amic acid had been formed, however, a comparison of the ^{1}H NMR spectrum of the crude product obtained from this reaction and a pure sample of the amic acid (**13**) obtained later via an alternative method (Section 2.2.8) clearly demonstrated that this assumption was incorrect.

study of these compounds; however, it was felt that further investigations into more general methods for the synthesis of these types of aryl imides would be very useful for several reasons. High pressure reactors are still not commonly available in organic chemistry laboratories and so general methods, if they could be found, would be much more practical and convenient. Also, a disadvantage in using the high-pressure reactor was that the reaction vessels used were necessarily small (~4.5 mL) limiting the scale of synthesis.

2.2.4.3 Further Exploration of Reaction Conditions with Anhydride (2)

A number of different reaction conditions were tested using 4-*tert*-butylaniline and (**2**). It was found, as with anisidine, that the desired amic acid was not easily formed. No amic acid was produced either by using temperatures ranging from ambient to 84°C, by heating the reactants neat at higher temperatures, by addition of catalytic amounts of acid or base, or by the use of a dehydrating agent (DCC) at room temperature and at 62°C.

In light of the reported ease of formation of similar amic acids from primary alkyl amines and (**2**)[3] it seemed that the failure to produce the aryl amic acids from either of these two aryl amines was due to their relatively weak nucleophilicity. Thus it was decided to try a new method leaving the anhydride (**2**) aside and using a more reactive alternative.

Interestingly, an almost identical aryl imide system was found in the literature whilst this work was in progress.[19,20] Unfortunately, no experimental details were included except a reference to an earlier paper that gave little information regarding the synthesis of the particular aryl imide in question.[21]

2.2.4.4 Reactions with the *Exo,Exo-Bis*-Acyl Chloride (11)

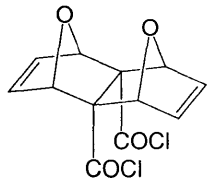

(**11**)

A search of the literature revealed that the *exo,exo*-fused *bis*-oxabridged norbornene *bis*-acyl chloride (**11**) had already been reported and, in fact, was used as an intermediate in an alternative synthesis of (**2**).[22] This compound was easily made by the published method and good yields (~70%) were obtained on a multi-gram scale. The ^{1}H NMR spectrum of the crystalline brown coloured solid obtained was in accordance with published spectra except that, whereas the two signals in the original work were measured as singlets, better resolution of the spectrum obtained in this work showed the signals to be poorly resolved multiplets.

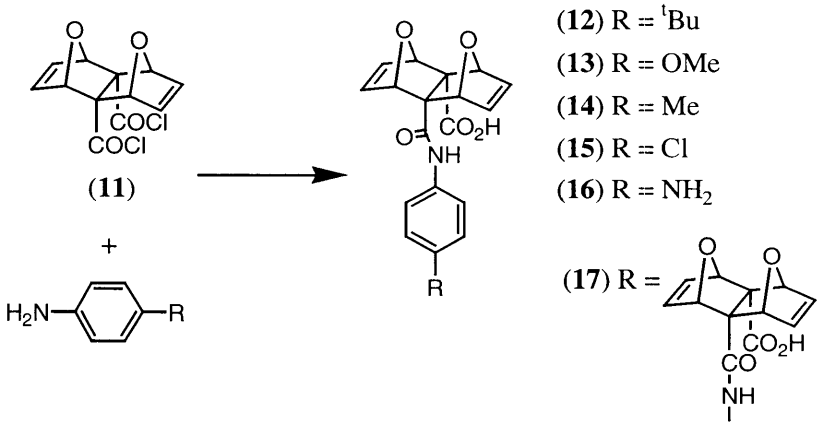

Scheme 2.4 Synthesis of aryl amic acids (**12-17**) from *bis*-acyl chloride (**11**).

Table 2.4 Reactivity of aniline derivatives with anhydride (**2**) and *bis*-acyl chloride (**11**).

Reactants (ratio)	Solvent (Reagents)	Temp. (°C)	Pressure (bar)	Time (hrs)	Yield (%) amic acid
(2):4-methoxyaniline (1:1)	$CHCl_3$	R.T	1*	168	0
	$CHCl_3$	60	1	24	0
	$CHCl_3$	100	1	48	0
	CH_2Cl_2	R.T	7000	24	trace
	CH_2Cl_2	R.T	13000	72	45[§]
(2):4-*t*-butylaniline (1:1)	CH_2Cl_2	R.T	1	24	0
	CH_2Cl_2	40	1	12	0
	$CHCl_3$	62	1	144	0
	1,2-DCE	84	1	8	0
	neat	180	1	0.5	0
	$CHCl_3$(DCC)	R.T	1	46	0
	$CHCl_3$(DCC)	62	1	144	0
(11):4-*t*-butylaniline (1:1)	$CHCl_3$	R.T	1	72	85 (**12**)
(11):4-methoxyaniline (1:1)	$CHCl_3$	R.T	1	72	43-68[¶] (**13**)
(11):4-methylaniline (1:1)	$CHCl_3$	R.T	1	72	85 (**14**)
(11):4-chloroaniline (1:1)	$CHCl_3$	R.T	1	72	63 (**15**)
(11):1,4-phenylenediamine (1:1)	$CHCl_3$	R.T	1	72	50 (**16**)
(11):1,4-phenylenediamine (2:1)	$CHCl_3$	R.T	1	72	59(dimer)(**17**)

*atmospheric pressure (not measured)

[§]yield of imide after dehydration with $NaOAc/Ac_2O$

[¶]yields from two separate runs

Stirring (**11**) with 4-*tert*-butylaniline in $CHCl_3$ under N_2 for 3 days in darkness gave the desired amic acid (**12**) in high yield (85%) after work up. To test the generality of the method a number of different aniline derivatives were reacted with (**11**) under identical conditions (Scheme 2.4 and Table 2.4). A series of amic acids (**12-17**) were obtained in this manner in moderate to good yields. One interesting result was the formation of the *bis*-amic acid phenylene-bridged dimer (**17**).

Although similar quantities of (**11**) could be produced in less than half the time taken to make the anhydride (**2**), it was much more difficult to handle with respect to stability and storage. Whereas large quantities of (**2**) were stored over long periods under dry conditions it was necessary to handle (**11**) under an inert atmosphere and use it as soon as it was made because it was prone to rapid decomposition in air at room temperature. Several grams of (**11**) were stored under nitrogen and refrigerated for several days with only a small loss in reactivity measured by a lower yield of amic acid product. The *bis*-acyl chloride (**11**) was converted to the anhydride (**2**) by treating it with a phosphate buffer solution using the method described in the literature.[22]

2.2.4.5 Conversion of Aryl Amic Acids to Imides

Treatment of amic acids (**12-15**) with sodium acetate (NaOAc) in acetic anhydride (Ac_2O) at 60°C or 100°C for extended periods (1-7 days) led to almost quantitative recovery of the starting compounds, after workup, with no formation of the respective imides detectable by ^{1}H NMR spectroscopy. Treatment of (**12**) with NaOAc and Ac_2O, at 120°C for 2 hours, gave a mixture of amic acid (**12**) and imide (**20**) in a ratio of ~2:1 after chromatographic separation whereas at a higher temperature (130°C) the imide (**20**) was isolated in 81% yield. Similar results were obtained for the conversion of (**13**) into (**21**) (T = 130°C, t = 3 hrs, 84%). Generally conversion of amic acid into imide was easily monitored by ^{1}H NMR spectroscopy of the crude product (Figure 2.10). It was found, however, that the use of the NaOAc/Ac_2O dehydration method for converting these amic acids into the respective imides proved to be more difficult than expected. In the cases where this method was used successfully it was found that the results were not easily reproduced and the percentage of amic acid converted to the imide varied markedly using the same reaction conditions and reaction times.

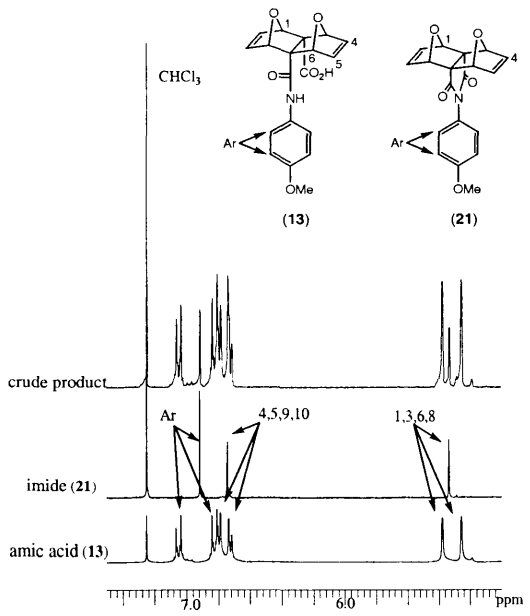

Figure 2.10 Monitoring amic acid conversion to imide using ^{1}H NMR spectroscopy. The example is of a 20% conversion of (**13**) into (**21**) as measured by integration of the amic acid and imide signals*.

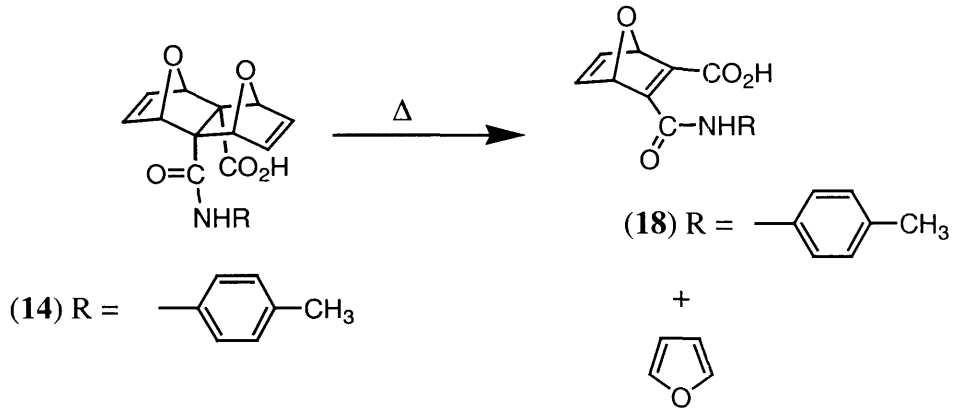

Scheme 2.5 Retro Diels-Alder degradation of amic acid (**14**) into (**18**) and furan.

* Note the atypical aryl singlet for (**21**) due to the accidental equivalence of chemical shifts for each pair of aromatic protons. All other aryl imides synthesised gave an AA'XX' multiplet for the aryl protons (23) Kemp, W. In *Organic Spectroscopy*; 3rd ed.; The Macmillan Press Ltd: London, 1991, p 158.

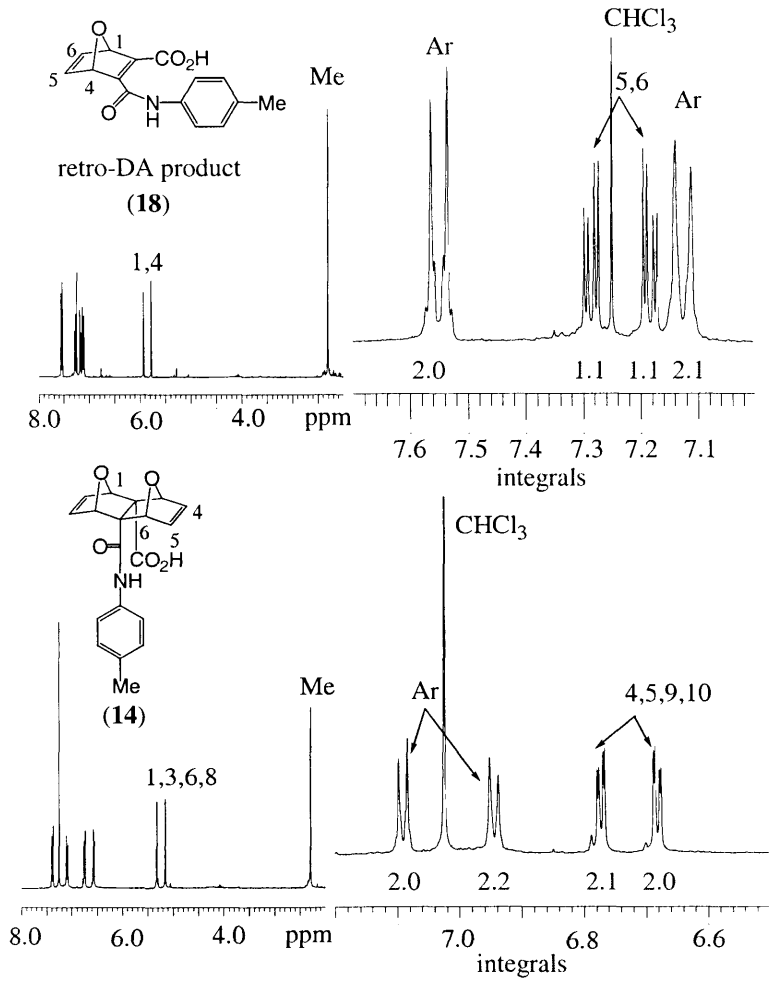

Figure 2.11 ^{1}H NMR spectra of (**14**) and its thermal degradation product (3-p-tolylcarbamoyl-7-oxa-bicyclo[2.2.1]hepta-2,5-diene-2-carboxylic acid) (**18**).

The NaOAc/Ac_2O method failed to give the corresponding imides from amic acids (**14-15**) at temperatures above 120°C. ^{1}H NMR analysis of each reaction mixture revealed that no imides had formed but, instead, decomposition of the amic acids had occurred. It was known that the *bis*-oxabridged norbornene diester analogue also degraded at relatively low temperatures via a retrograde Diels-Alder (retro-DA) pathway.[3,24] The spectra of the crude reaction mixtures were consistent with products obtained from a retro-DA reaction. In particular the retro-DA product (3-p-tolylcarbamoyl-7-oxa-bicyclo[2.2.1]hepta-2,5-diene-2-carboxylic acid) (**18**) from (**14**) was obtained in high yield (85%) after chromatographic purification (Scheme 2.5 and Figure 2.11). In all these dehydration reactions it seems there is a competition between the ring closing imide formation and the thermally induced loss of a furan ring via a retro-DA reaction. The energy required to form the imide may be lower than the energy required to break the C_2-C_3 and C_6-C_7

bonds in the cases of both (**12**) and (**13**) and vice versa for (**14**) and (**15**)*. It was uncertain whether this was mainly due to a difference in the nucleophilicity of the respective amide nitrogens caused by the electron donating or withdrawing nature of the aryl *para*-substituents, or a difference in the thermal stabilities of each amic acid or, indeed, both.

In order to further investigate the retro-DA degradation process and the relative stabilities of each of the amic acids (**12–15**) a series of NMR experiments were performed at temperatures ranging from 30°C to 150°C in d_6-DMSO. After obtaining a ^{1}H NMR spectrum of each of the amic acids at 30°C the temperature of each sample was increased by increments of 10°C and NMR spectra obtained at each temperature up to a maximum of 150°C. The samples were ssheld at each temperature for 2 minutes before a spectrum was acquired (acquisition time = 1 min 20 s). Each of the amic acids (**12–15**) was found to degrade at high temperatures. The presence of the respective retro-DA products (**18-21**) and furan were detected in all cases. The methyl substituted amic acid (**14**) was found to be the least stable at raised temperatures and began to degrade at 120°C with no amic acid (**14**) being detected at 150°C (Figure 2.12). Amic acids (**12**) and (**13**) underwent retro-DA degradations at 130°C and approximately 20% of (**12**) remained at 150°C with none of the methoxy substituted amic acid (**13**) being found at the same temperature. Amic acid (**12**) completely degraded after being held at 150°C for a further 5 minutes. The chlorophenyl amic acid (**15**) remained stable up to a temperature of 130°C and approximately 25% of (**15**) remained at 150°C with complete degradation being found after a further 5 minutes at this temperature.

As all the amic acids (**12-15**) tested underwent retro-DA degradations at similar rates above 130°C it can be concluded that the overriding factor in their ability to form the respective imides using the NaOAc/Ac_2O method is related to the relative nucleophilic strength of the amide nitrogen. Thus, even though (**15**) was found to be one of the most thermally stable in d_6-DMSO it failed to form the imide (**25**) under the NaOAc/Ac_2OAc dehydration conditions.

It was then considered that performing the NaOAc/Ac_2O dehydration reaction in a sealed tube might prevent the loss of furan by shifting the equilibrium toward the reactant side under high pressure conditions. This idea was tested using the least stable amic acid (**14**) both in the presence and absence of an excess of furan. Without adding furan it was found from NMR analysis, after a 3 hour reaction time, that the crude reaction product consisted of a 9:1 ratio of amic acid (**14**)

---

* Compounds (**16**) and (**17**) were not tested at temperatures above 60°C.

starting material to imide (**24**). Repeating this reaction for a longer period (24 hrs) led to significant degradation of the amic acid as evidenced by an NMR analysis of the crude reaction product. Only a low yield (10%) of the imide (**24**) was obtained after work-up. In the presence of an excess of furan a significant amount of imide had formed under the sealed tube conditions after 3 hrs but a number of unknown peaks in the NMR spectrum of the crude mixture indicated that competing side reactions were also taking place and this was reflected in the low yield of (**24**) (20%) being obtained after work-up. Unfortunately the sealed tube method was unsatisfactory for the synthesis of the imides due to the combination of low yields and comparatively small scales dictated by the size of the reaction vessels available.

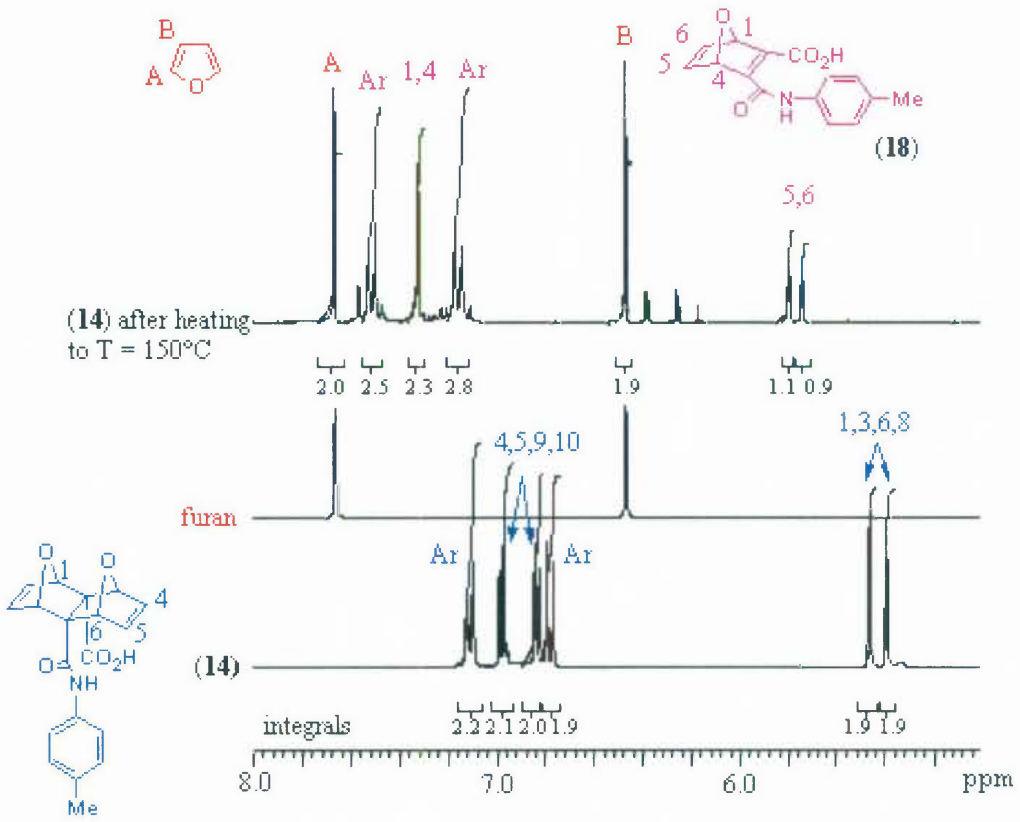

Figure 2.12 ^{1}H NMR analysis of the thermal degradation of (**14**) in d_6-DMSO demonstrating clearly the loss of furan via a retro-DA process.

The challenge was to find a method that promoted the formation of the imide at low enough temperatures in order to avoid the retro-DA reaction. This was most important for aryl

amic acids containing either a weak electron donating [e.g. (**14**)] or electron withdrawing substituent [e.g. (**15**)]. A widely used method for the formation of esters and amides under mild conditions is the use of the dehydrating agent 1-(3-dimethylaminopropyl)-3-ethylcarbodiimide hydrochloride (EDC) in conjunction with 1-hydroxybenzotriazole (HOBT), which acts as an activator by forming an activated ester intermediate. These reagents were used in subsequent preparations.

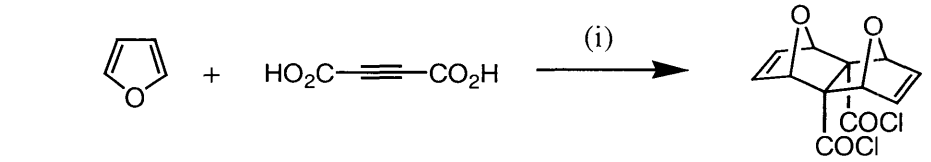

(**11**) 67%

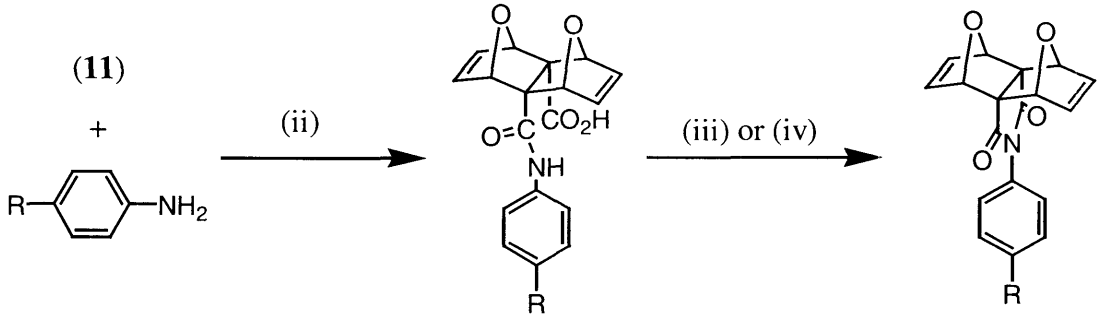

(**12**) R = ^{t}Bu 85%
(**13**) R = OMe 43-68%
(**14**) R = Me 85%
(**15**) R = Cl 63%
(**16**) R = NH_2 50%

(**17**)* R = 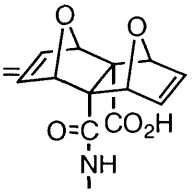 59%

(**20**) R = ^{t}Bu 81% (iii), 80% (iv)
(**21**) R = OMe 84% (iii) 70% (iv)
(**22**) R = Me 72% (iv)
(**23**) R = Cl 60% (iv)

(**24**) R= 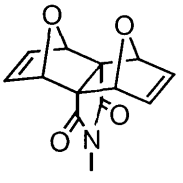 40% (iv) from (**17**)

* The phenylene-bridged dimer (**17**) was formed from a 1:2 ratio of 1,4-phenylene diamine and (**11**) in CH_2Cl_2/diethyl ether (1:1)

Scheme 2.6 General synthetic route toward *bis*-oxabridged norbornene aryl imides. Reagents and Conditions: (i) PCl_5, R.T, N_2 atm, CCl_4, 7 days (ii) R.T, N_2 atm, CH_2Cl_2, 2 days (iii) NaOAc/Ac_2O, T=130°C, 2-6 hrs (iv) EDC/HOBT, R.T, N_2 atm, THF(dry) 3 days.

The amic acids (**12-15**) and (**17**) were all converted to the respective imides (**20-24**) in moderate to good yields by stirring with EDC/HOBT in dry THF under N_2 for 3 days at room temperature (Scheme 2.6). The identity of the amic acids and imides were easily obtained from the respective ^{1}H NMR spectra, which reflected the difference in symmetries of these compounds as shown earlier in Figure 2.10. The aryl amic acids typically gave: an AA'XX' type multiplet for the aromatic protons at around 7 ppm; two distinct and strongly coupled signals at around 6.8 ppm for each pair of alkene protons (H_4,H_{10} and H_5,H_9); and two signals at around 5.3 ppm for the chemically distinct pairs of oxa-bridge protons (H_1,H_3 and H_6,H_8). The more highly symmetrical imides had a triplet (^3J = 0.9 Hz) for each set of four equivalent alkene and oxa-bridgehead protons. Accurate masses (EI) were obtained for all the aryl imides except (**21**)*.

In summary; a general two-step method was eventually developed for the formation of aryl imide derivatives of the fused *bis*-oxabridged norbornene starting from the *bis*-acyl chloride (**11**) and various *para*-substituted anilines. A new phenylene-bridged fused *bis*-oxabridged norbornene dimer (**24**) was also synthesised using this method and has potential use for the production of higher order systems such as porphyrin tetramers but the extension and coupling of such double-bridge systems was not investigated further. The aim of these experiments was to find generally applicable methods for the production of the desired imides and the yield for each particular imide synthesis was, therefore, not optimised. The key to successfully synthesising a range of different aryl imides was to find a mild enough method for dehydration of the amic acids so as to avoid the thermal retro-DA degradation.

2.2.5 AN ALKYL IMIDE – FLEXIBLE TETHER

The synthesis of an alkyl imide derivative from the reaction of 2-(2-ethoxyethanolamine) with the anhydride (**2**) offered a way of introducing an alcohol or alcohol derivative within the cavity of a PSP attached to a flexible tether. The hydoxyl group could potentially act as a covalently attached ligand for binding with a metal centre, a hydrogen-bonding site, a proton transfer group in a host-guest or catalytic system, or an attachment point for an electron acceptor or other unit. A fully extended structure of the covalently attached hydroxyl group, within the cavity of a proposed PSP, is shown in Figure 2.13.

---

* An accurate mass was obtained for the *bis*-cyclobutene extended derivative (**27**).

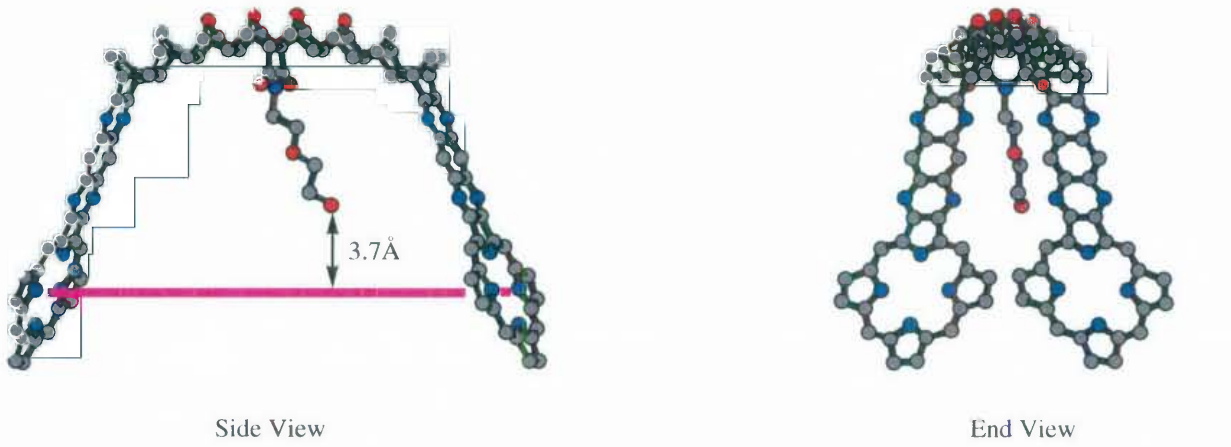

Figure 2.13 Molecular model (AM1) of the skeletal structure of a proposed PSP with a fully extended flexibly tethered hydroxyl group. Static distance (3.7 Å) = the distance between the hydroxyl hydrogen and the inter-porphyrin plane (pink line).

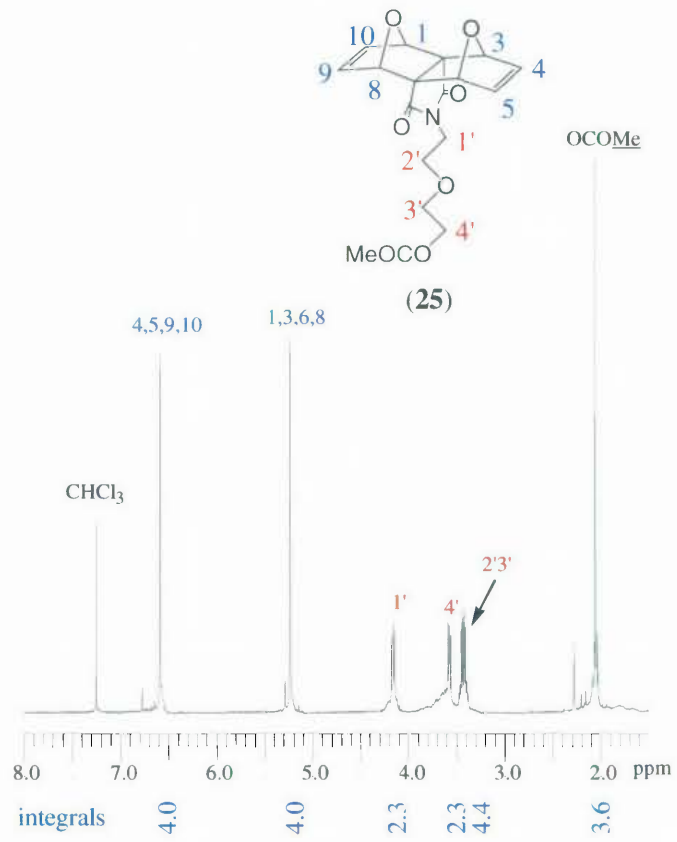

Figure 2.14 ^{1}H NMR spectrum of imide (**25**).

2-(2-ethoxyethanolamine) reacted with (**2**) at room temperature giving the expected amic acid intermediate. The amic acid proved difficult to separate from the ethoxyethanolamine starting material by chromatography so the impure product was treated with $NaOAc/AC_2O$ at 60°C for 3 days. The alcohol group was also esterified under these conditions and so the imide (**25**) was

formed, albeit in relatively low yield (20%), and was obtained as a viscous brown oil which gave a ^{1}H NMR spectrum consistent with the proposed structure (Figure 2.14).

2.3 EXTENDED IMIDE BUILDING BLOCKS: *BIS*-CYCLOBUTENE DIESTERS AND *BIS*-EPOXIDES

The extension of norbornene and hetero-norbornene systems via ruthenium-complex catalysed [2+2] cycloadditions with dimethylacetylene dicarboxylic acid (DMAD) was first reported over two decades ago and is now more generally referred to as the Mitsudo reaction.[25] As discussed in the previous Chapter (Section 1.4.2), this method has proven to be valuable for the synthesis of various *exo*-cyclobutene adducts formed from cyclisation with DMAD and a number of other acetylene derivatives.[26,27] $[Ni(PPh_3)_2Cl_2]/PPh_3/Zn$ and $[Co(PPh_3)_2I_2]/PPh_3/Zn$ systems have also been reported recently to act as catalysts for a variety of [2+2] cycloadditions between alkynes and oxa- or azabenzonorbornadienes.[28,29] For the pathway outlined in Scheme 2.7, the ruthenium complex catalyst, $RuH_2CO(PPh_3)_3$, was prepared according to literature methods and its identity verified inter-alia by its IR spectrum (ν_{CO} = 1940 cm^{-1}, ν_{RuH} = 1960 cm^{-1} and 1900 cm^{-1}).[30] The *bis*-cyclobutene diester adducts (**26-28**) were prepared from the consecutive cycloadditions of two equivalents of DMAD to the respective imides (**20**, **21** and **25**) (Scheme 2.7).

The products were easily identified from their ^{1}H NMR spectra where a new signal for the protons at positions 4,7,10 and 14 of the extended imides **26-28** (Scheme 2.7) arises at ~3.2 ppm in place of the alkenyl protons at positions 4,5,9 and 10 (~6.7 ppm) of the starting compounds (**20**, **21** and **25**) along with a strong signal at ~3.8 ppm for the methyl ester protons. The oxa-bridge protons resonate upfield in comparison to the starting compounds (~4.8 ppm compared to ~5.3 ppm) due to the removal of the deshielding effects from the neighbouring double bond. In all three [2+2] cycloaddition reactions the major by-product was benzene-1,2,3,4,5,6-hexacarboxylic acid hexamethyl ester which was formed from the competing cyclotrimerisation of DMAD. The presence of the hexaester by-product was easily identified by a sharp ^{1}H NMR signal at 3.87 ppm. Accurate masses (EI) were obtained for the three cyclobutene adducts (**26-28**). The poor yield of **(28)** is noteworthy and may be due to competitive binding of the Ru catalyst to oxygen atoms of the reactant, although this was not investigated further.

References, p. 106

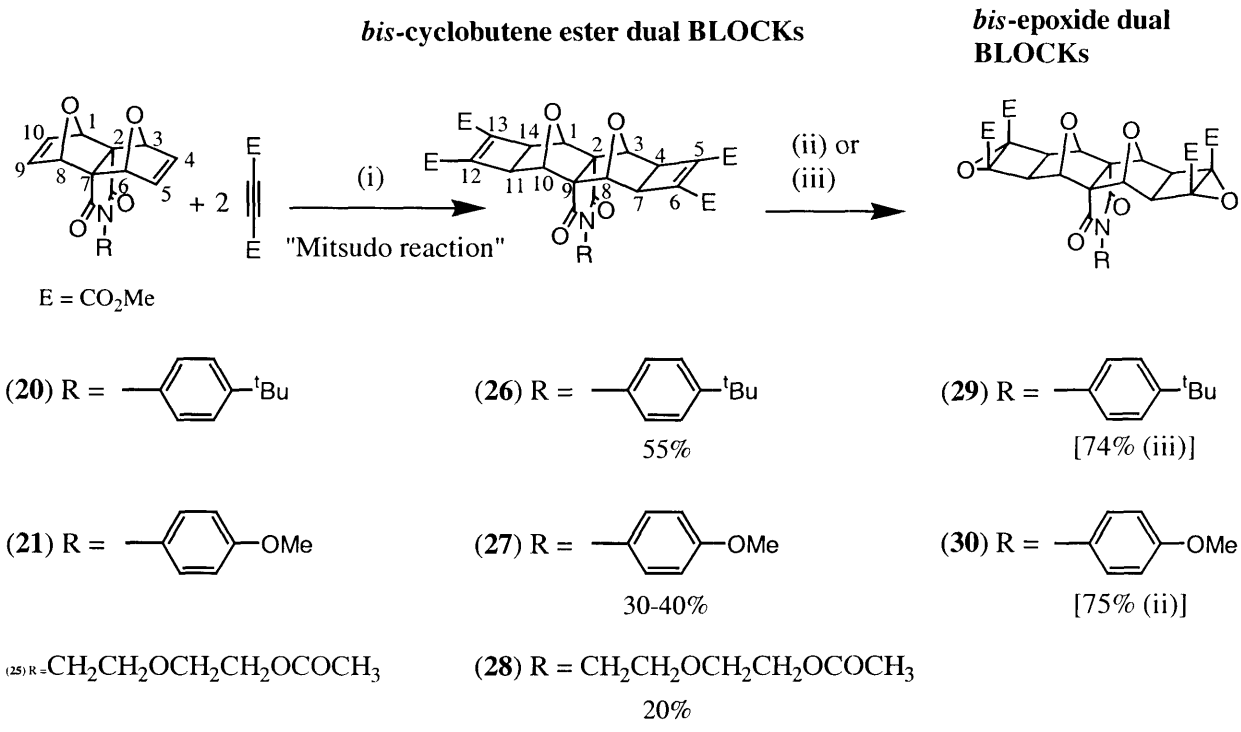

Scheme 2.7 Extended aryl imide building blocks via Ru(0) catalysed [2+2] cycloaddition and epoxidation reactions. Reagents and Conditions: (i) 2% $RuH_2CO(PPH_3)_3$, 80°C, benzene, 4 days (ii) ^tBuOOH, MeLi, -78°C to 20°C, N_2 atm, THF (dry), 6.5 hrs (iii) ^tBuOOH, ^tBuOK, -5 to 15°C, N_2 atm, THF (dry), 4 hrs.

The alternative route to a *bis*-cyclobutene diester via ruthenium catalysed [2+2] cycloaddition of the amic acid and subsequent cyclisation to the imide using $NaOAc/Ac_2O$ was attempted (Scheme 2.8).

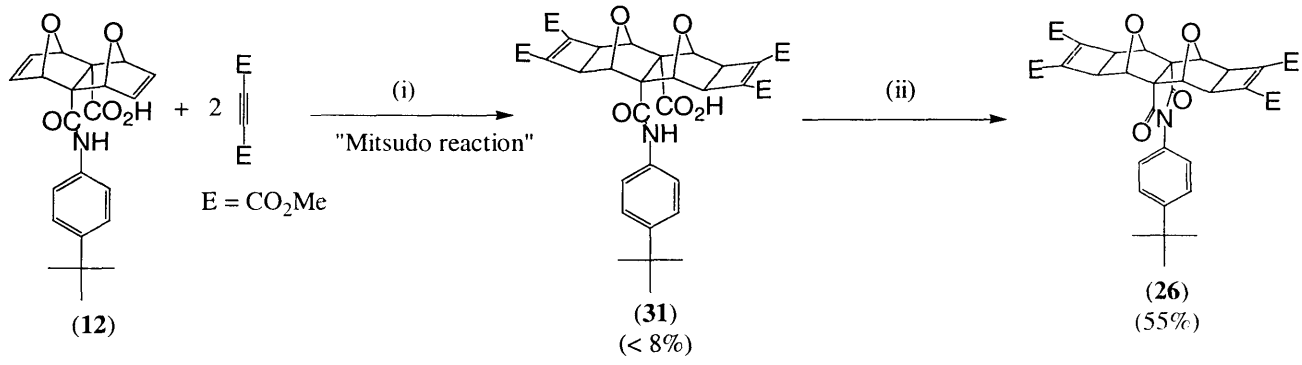

Scheme 2.8 Alternate route toward *bis*-cyclobutene diester imides. Reagents and Conditions: (i) 10% $RuH_2CO(PPH_3)_3$, 80°C, benzene, 4 days (ii) $NaOAc/Ac_2O$, 130°C, 12 hrs.

This route was considered after the thermal instability of the amic acids became evident. It was thought that fusion of the *bis*-oxa-norbornene tetracycle to the cyclobutene rings would effectively block the retro-DA degradation pathway. It was considered that the resulting *bis*-cyclobutene diester amic acid could then be dehydrated using the usual $NaOAc/Ac_2O$ method at raised temperatures. The aryl amic acids (**12-13**) were submitted to 'Mitsudo' reaction conditions [10% $RuH_2CO(PPh_3)_3$] and crude products analysed. Thin layer chromatography (silica) revealed a complex mixture of products had formed in each case and only very small amounts of the *bis*-cyclobutene diester products were detectable by ^1H NMR spectroscopy. A dominant singlet at 3.87 ppm indicated that the main product forming in all cases was the benzene hexaester. The best result was for the cycloaddition to (**12**). Further purification of (**12**) using flash column chromatography gave a product with a ^1H NMR spectrum consistent with the *bis*-cyclobutene diester amic acid (**31**). The yield of (**31**) was very low (less than 8%) showing that this was not an efficient method for the synthesis of *bis*-cyclobutene imides, especially in comparison with the relative success of the previous route. Nevertheless, the identity of (**31**) was established by converting it to (**26**) by the $NaOAc/Ac_2O$ method (55%).

Two *bis*-epoxide derivatives (**29-30**) were prepared in equally good yields (~75%) using either ^{t}BuOOH* and MeLi at -78°C or ^{t}BuOOH and ^{t}BuOK at -5°C, both carried out in dry THF under an inert atmosphere (Scheme 2.7).[31] The ^1H NMR spectral pattern of the epoxides is very similar to that obtained from the cyclobutene esters. Changes in the chemical shifts of the oxa-bridge protons ($\Delta\delta \sim +0.75$ ppm) and the cyclobutane protons ($\Delta\delta \sim -0.36$ ppm) were observed. The *bis*-cyclobutenes (**26-28**) and *bis*-epoxides (**29-30**) are new centrally functionalised building blocks that can be joined to other complementary building blocks via either [4+2] Diels-Alder, transition metal catalysed [2+2], or [3+2] 1,3-dipolar cycloadditions. In particular the *bis*-epoxides are ideal for the production of arched PSPs (*vide infra*).

2.4 PORPHYRIN BUILDING BLOCKS

2.4.1 EXTENSION OF CROSSLEY'S PORPHYRIN QUINOXALINO-DIAMINES

---

* A 3.8M solution of ^{t}BuOOH in toluene was prepared according to literature methods and the concentration calculated from the ^1H NMR spectrum. (31) Hill, J. G.; Rossiter, B. E.; Sharpless, K. B. *J. Org. Chem.* **1983**, *48*, 3607.

The porphyrin blocks (PBlocks) used in this work were based on the porphyrin α-diones developed by Crossley and co-workers.[32] Extension of the porphyrin α-dione* (**37**), via coupling with 1,2,4,5-benzenetetramine and then coupling the resultant porphyrin-quinoxalino-diamine (**38**) with another α-dione, has been used to produce a number of β-fused multi-porphyrin systems including the homo-coupled dimer (**40**).[33-37] The *tetrakis*-(3,5-di-*tert*-butylphenyl)PBlock (**39**) (^{t}BuPBlock), developed by Warrener's group, has previously been synthesised by coupling (**38**) with a fused polycyclic norbornene dione (**7**) (Scheme 2.9).[38]

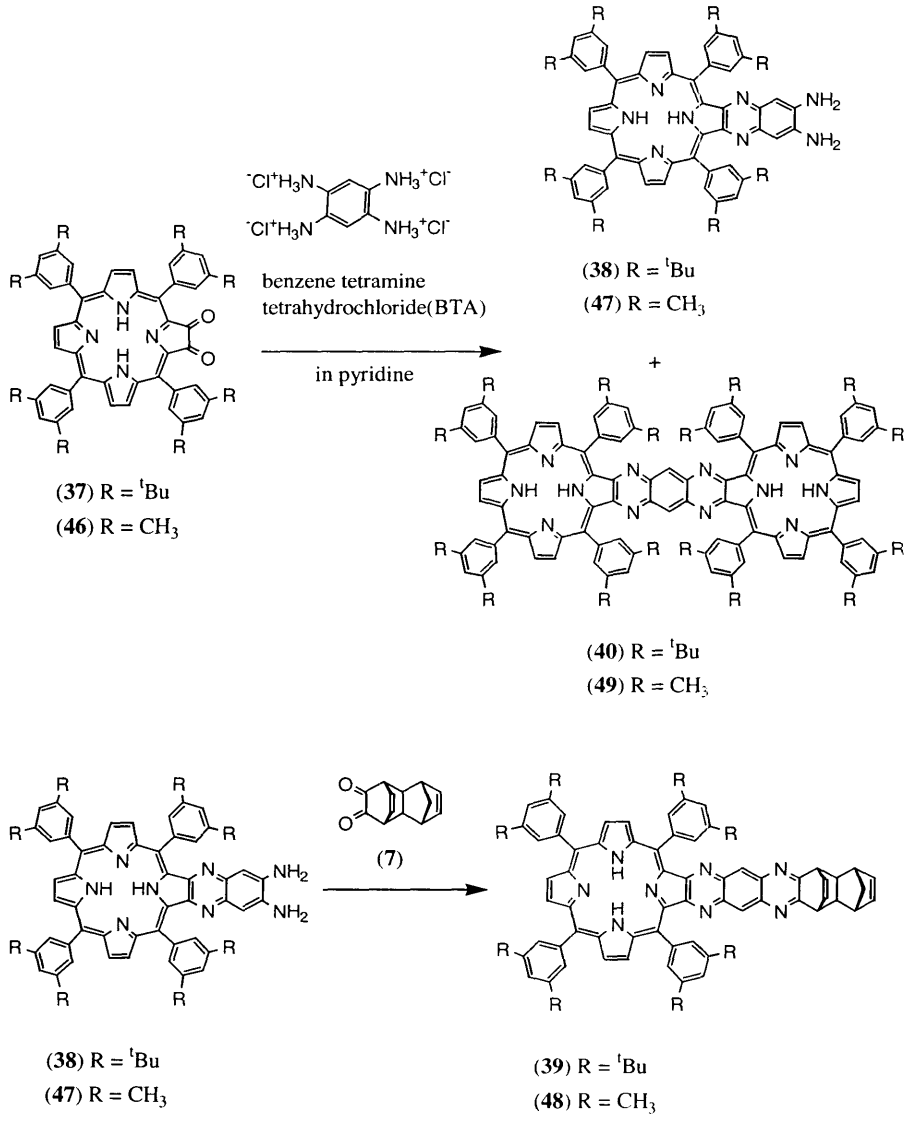

Scheme 2.9 General synthetic approach toward porphyrin blocks (PBlocks).

* Alternatively these compounds can be described as '2,3-diketo-porphyrins', '2,3-dioxo-porphyrins' or '17,18-dioxo-chlorins'.

A number of *bis*-porphyrin systems, of different shapes and sizes, has been reported recently using coupling reactions of (**39**) with various spacer groups, thus demonstrating the versatility of this building block.[38-45] In conjunction with the development of these systems it was decided to synthesise a new porphyrin block (**48**) (MePBlock) starting from 2,3-dioxo-5,10,15,20-*tetrakis*-(3,5-dimethylphenyl)porphyrin (**46**) rather than (**37**) (Scheme 2.10). The use of PBlocks with different peripheral groups attached to the porphyrin ring would allow added design flexibility as both the electronic characteristics of the porphyrin sub-unit and the binding strength of metallated derivatives can be, in principle, tuned or modulated in this manner. Smaller peripheral groups on the porphyrin ring, as in (**46**), may also be useful in future development of porphyrin systems where more accessible cavities are needed, or to avoid steric crowding by bulky *tert*-butyl groups. The previously described ^{t}BuPBlock (**39**) was also used as part of this work so that comparisons between it and the new targeted MePBlock (**48**) could be made.

2.4.2 SYNTHESIS OF 5,10,15,20-*TETRAKIS*-(3,5-DIMETHYLPHENYL)-PORPHYRIN BLOCK (**48**) (MePBlock)

The synthesis of (**48**) was carried out following the general methods reported by Crossley and co-workers (Scheme 2.10).[32,46,47] 5,10,15,20-*tetrakis*-(3,5-dimethylphenyl) porphyrin (**41**) was synthesised from 3,5-dimethylbenzaldehyde and pyrrole in 18% yield using the Adler method and it was established that the optimal reaction time was 2.5 hrs. It was also found that it was essential that both the aldehyde and pyrrole were pure otherwise very low yields of this tetraphenyl porphyrin were obtained.

The aldehyde itself was prepared from mesitylene in two steps. Photo-initiated bromination of mesitylene using a stoichiometric amount of N-bromosuccinimide resulted in unwanted dibrominated products so an excess of mesitylene was used. The resulting mixture of mesitylene and 1-bromomethyl-3,5-dimethylbenzene was submitted to Sommelet reaction conditions giving a mixture of the desired aldehyde and unreacted mesitylene. The pure aldehyde was easily separated from this mixture by formation, aqueous extraction and subsequent base promoted decomposition of a bisulfite addition complex.

Quantitative conversion of 5,10,15,20-*tetrakis*-(3,5-dimethylphenyl)porphyrin (**41**) to [5,10,15,20-*tetrakis*-(3,5-dimethylphenyl)porphyrinato]copper(II) (**42**) was achieved by heating with $Cu(OAc)_2 \cdot H_2O$ in $CHCl_3$/MeOH. Nitration of the copper(II) complex at the β-position using a NO_2/hexane solution (0.32 g in 20 mL hexane) was followed by demetallation (conc. H_2SO_4)

and then reduction of the free-base nitro-porphyrin (**44**) to the photosensitive porphyrin β-amine (**45**).

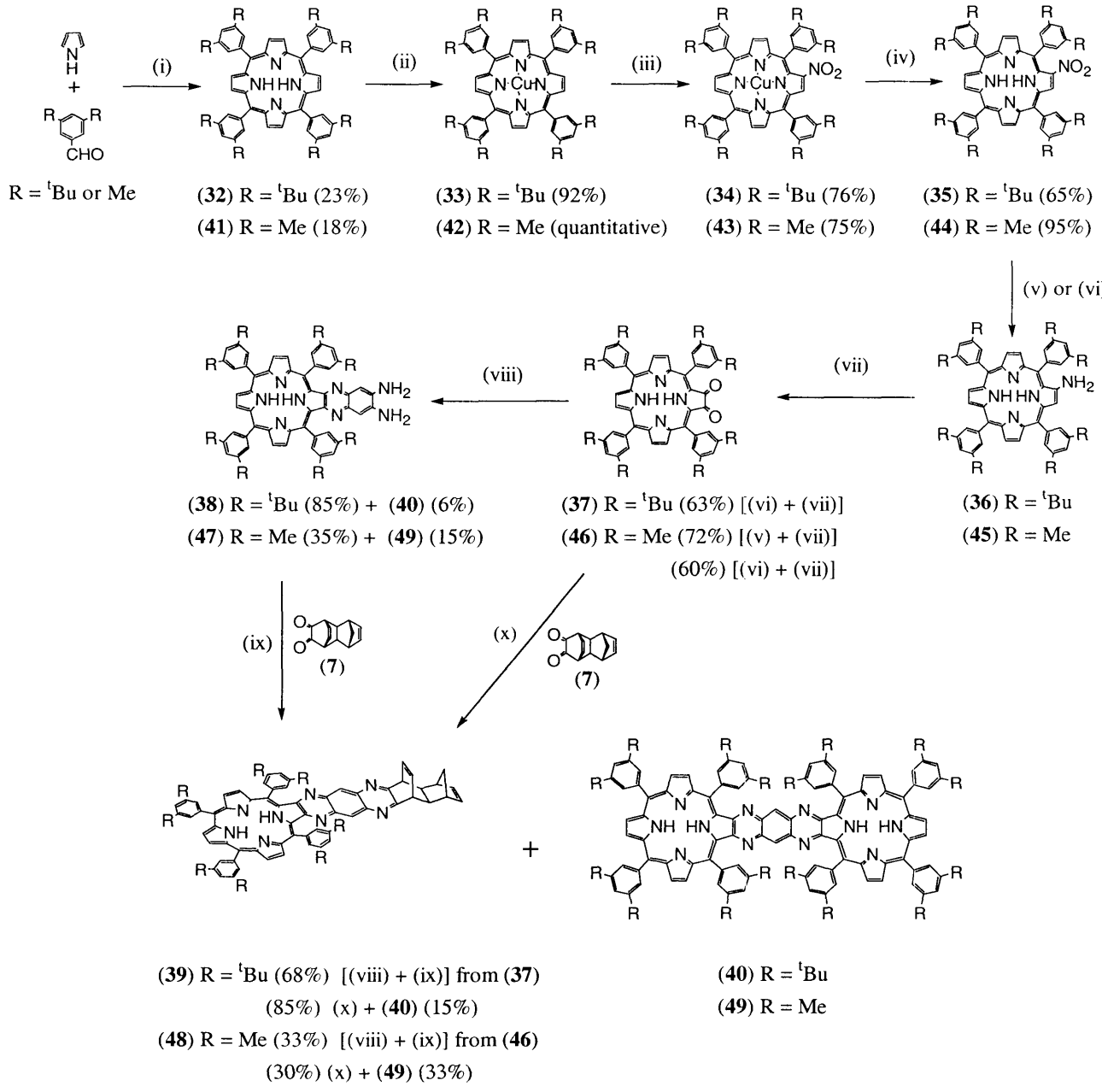

Scheme 2.10 Total synthesis of *tetrakis*-(3,5-di-tert-butylphenyl) porphyrin block (**39**) and *tetrakis*-(3,5-dimethylphenyl) porphyrin block (**48**). Reagents and Conditions: **R = Me** (i) Δ, propionic acid, 30 min. (ii) $Cu(OAc)_2.H_2O$, Δ, $CHCl_3$/MeOH, 24 hrs (iii) NO_2/hexane (0.32g/20ml), 0°C, $CHCl_3$, (iv) conc. aq H_2SO_4, R.T, $CHCl_3$, 20 min. (v) $SnCl_2.H_2O$ / conc. aq HCl, R.T, $CHCl_3$, 2 days (vi) $NaBH_4$, 10%Pd/C, R.T, N_2 atm, CH_2Cl_2, 6 hrs (vii) hν, O_2, R.T, $CHCl_3$, 24 hrs then add dil. aq HCl, R.T, 1 hr (viii) benzenetetramine tetrahydrochloride, R.T, N_2 atm, pyridine, 36 hrs (ix) (**7**), R.T, N_2 atm, $CHCl_3$, 24 hrs then Δ at 60°C, 2 hrs (x) benzenetetramine tetrahydrochloride, Δ at 60°C, N_2, pyridine, 1 hr then add (**7**), Δ at 60°C , 8 hrs. **R = tBu** (i) Δ, propionic acid, 2.5 hrs (ii) $Cu(OAc)_2.H_2O$, Δ, $CHCl_3$/MeOH, 12 hrs (iii) NO_2/hexane (0.32g/20ml), 0°C, CH_2Cl_2 (iv) conc. aq H_2SO_4, R.T, CH_2Cl_2, 20 min. (vi) $NaBH_4$, 10%Pd/C, R.T, N_2 atm, CH_2Cl_2, 2 hrs (vii) hν, O_2, R.T, CH_2Cl_2, 24 hrs then add dil. aq HCl, R.T, 1 hr (viii) benzenetetramine tetrahydrochloride, R.T, N_2 atm, pyridine, 14 days (ix) (**7**), R.T, N_2 atm, CH_2Cl_2, 3 days then Δ at 60°C, 3 hrs (x) benzenetetramine tetrahydrochloride, N_2, Δ at 60°C, pyridine, 1 hr then add (**7**), Δ at 60°C, 8 hrs.

The reduction was carried out using either acidified stannous chloride or sodium borohydride with 10% Pd/C. The crude porphyrin amine was photo-oxidised to the porphyrin α-dione (**46**) with $O_{2\,(g)}$ and visible light and the yield obtained was reasonably good when calculated from the nitro-porphyrin starting compound (72%). All the porphyrin intermediates were analysed by NMR and/or UV-Vis spectroscopic methods and the progress of each reaction was easily monitored using TLC. Purification of each porphyrin intermediate was achieved using a combination of flash column chromatography (silica) and recrystallisation from $CHCl_3$/MeOH.

The most significant and predictable difference between the two ^{1}H NMR spectra of the porphyrin diones (**37** and **46**) comes from the chemical shifts of the methyl substituents on the phenyl rings (Me proton signals at δ= 2.57 and 2.53 ppm compared with ^{t}Bu proton signals at δ= 1.50 and 1.46 ppm).

Addition of the porphyrin dione (**46**) to a stirred solution of benzenetetramine tetrahydrochloride (BTA) in pyridine, under an inert atmosphere, failed to give the desired fused diamino-quinoxalinoporphyrin (**47**) but instead led to the formation of the pyrazino[2,3-*g*]quinoxaline bridged porphyrin dimer (**49**) as the main product. The dimer (**49**) was easily identified from the simple ^{1}H NMR spectrum obtained, owing to its D_{2h} symmetry, and from the unusual pattern of two, almost equally strong, Soret bands [λ_{max} (log ε) ($CHCl_3$): 424(5.47), 456(5.40)] in the visible absorption spectrum. The two strong Soret bands are also explicable from symmetry considerations and an excitonic coupling mode and are in very close agreement to the spectral data published for the analogous *tetrakis*-(3,5-*tert*-butylphenyl) porphyrin dimer.[33] The presence of dimer (**49**) in the reaction mixture was easily identified by TLC analysis as it had the largest R_f value of all porphyrinic compounds present ($R_f \approx 0.5$, 1:1 petroleum spirit/$CHCl_3$). In order to promote the formation of the desired quinoxalino-diamine adduct (**47**) in favour of the dimer (**49**), a solution of porphyrin dione (**46**) was added dropwise to an excess of BTA in pyridine over several hours but once again the formation of (**49**) predominated. It was eventually discovered* that the rapid addition of a small excess of solid BTA to a stirred solution of (**46**) gave the highest yields of (**47**) (35%) after chromatographic purification with only a small amount of the unwanted dimer (**49**) being isolated (6%).

---

* A special acknowledgment is made to Dr. Martin Johnston for advice on solving this problem.

Table 2.5 Comparison of ^{1}H NMR data of porphyrin α-diones (**37**) and (**46**) with the fused quinoxaline adducts (**38**) and (**47**)*.

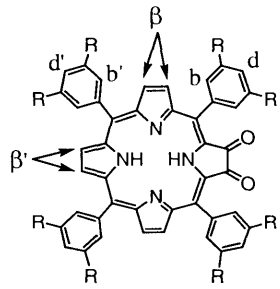

(**37**) R = ^{t}Bu
(**46**) R = CH_3

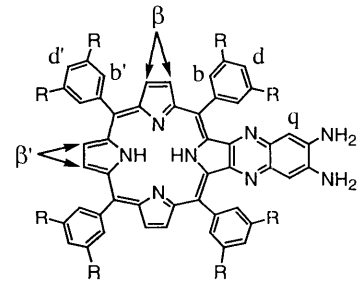

(**38**) R = ^{t}Bu
(**47**) R = CH_3

$CDCl_3$ 300MHz ref: ($CDCl_3$) 7.25	(**46**) R = CH_3 chemical shift (ppm)	(**47**) R = CH_3 chemical shift (ppm)	(**37**) R = ^{t}Bu chemical shift (ppm)	(**38**) R = ^{t}Bu chemical shift (ppm)
peak assignment¶	δ (#Hs) (multiplicity)	δ (#Hs) (multiplicity)	δ (#Hs) (multiplicity)	δ (#Hs) (multiplicity)
β	8.75 (2H) 8.62 (2H) (AB_q) J = 4.6 Hz	8.95 (2H) 8.90 (2H) (AB_q) J = 5.0 Hz	8.77 (2H) 8.60 (2H) (AB_q) J = 4.8 Hz	9.04 (2H) 8.99 (2H) (AB_q) J = 5.0 Hz
β'	8.57 (2H) (s)	8.71 (2H) (s)	8.61 (2H) (s)	8.81 (2H) (s)
b'	7.73 (4H) (s)	7.83 (4H) (s)	7.98 (4H) (d) J = 1.8 Hz	8.14 (4H) (d) J = 1.8 Hz
b	7.50 (2H) (s)	7.77 (4H) (s)	7.71 (4H) (d) J = 1.8 Hz	8.01 (4H) (d) J = 1.8 Hz
d	7.39 (2H) (s)	7.47 (2H) (s)	7.77 (2H) (t) J = 1.8 Hz	7.92 (2H) (t) J = 1.8 Hz
d'	7.36 (2H) (s)	7.40 (2H) (s)	7.74 (2H) (t) J = 1.8 Hz	7.82 (2H) (t) J = 1.8 Hz
q	–	7.05 (2H) (s)	–	6.97 (2H) (s)
NH_2	–	3.98 (4H) (bs)	–	3.94 (4H) (bs)
R	2.57 (12H) (s) 2.53 (12H) (s)	2.59 (24H) (s)	1.50 (36H) (s) 1.46 (36H) (s)	1.56 (36H) (s) 1.52 (36H) (s)
NH	-2.04 (2H) (bs)	-2.57 (2H) (bs)	-1.93 (2H) (bs)	-2.45 (2H) (bs)

* All data presented are from compounds synthesised as part of this study.
¶ see Scheme 2.10.

The porphyrin α-diones (**37** and **46**) and the porphyrin-quinoxalinodiamines (**38** and **47**) all have similar ^{1}H NMR spectra reflecting their similar symmetry (C_{2v}). The protons most affected by the introduction of an adjacent aromatic group in structures (**38**) and (**47**) are at the β-porphyrin [$\Delta\delta \approx$ +(0.2 - 0.3) ppm], aryl b [$\Delta\delta \approx$ +(0.2 - 0.3) ppm] and d ($\Delta\delta \approx$ 0.15 ppm) positions (Table 2.5).

Several grams of the key polycyclic dione (**7**) were prepared by the [4+2] cycloaddition of *o*-quinone (generated *in situ* from catechol and iodobenzene diacetate) and norbornadiene according to literature methods.[48] This dark yellow crystalline solid could be stored for long periods in a desiccator in darkness and gave a ^{1}H NMR spectrum, shown in Figure 2.16, in agreement with that of the literature.[23] Fine coupling (J = 0.88 Hz) between H_a and H_4 and negligible coupling between H_b and H_4 along with chemical shift differences due to the proximity of H_a to the neighbouring double bond (C_{11}-C_{12}) were used to distinguish between the NMR signals of the methylene bridge protons H_a and H_b.[49]

Stirring equal amounts of the quinoxalino-diaminoporphyrin (**47**) and dione (**7**) in dry deoxygenated pyridine, under N_2, for 19 hrs at R.T., followed by heating at 60°C for 2 hrs*, gave very high yields (up to 98%) of MePBlock (**48**). The synthesis of MePBlock (**48**) could also be carried out using a 'one-pot' method by adding BTA to a solution of porphyrin dione (**46**) and heating it for 3 hrs followed by the addition of dione (**7**) with continued heating overnight. The more convenient one-pot method gave only slightly lower yields (30%) compared with the two-step method (33% overall). The ^{1}H NMR, ^{13}C NMR, UV-Vis and Mass Spectral data of MePBlock (**48**) were all in accordance with the proposed structure. Assignments of all the ^{1}H NMR signals were supported by results from 2D COSY and 2D NOESY NMR analysis (Figure 2.15).

Due to the relative low yield of the quinoxalino-diamine derivative (**47**) (35%) compared to the 3,5-di-*tert*-butyl substituted analogue (**38**) (85%), an attempt was made to use a reverse order synthesis for MePBlock (**48**). It was planned to first form the quinoxalinodiamine adduct from (**7**) and then subsequently react it with the porphyrin dione (**46**). A single attempt at the synthesis of the quinoxalinodiamine derivative of dione (**7**), by addition of a stoichiometric amount of BTA to a solution of (**7**), however, led exclusively to the formation of the unwanted dimeric adduct (**50**), as evidenced by the ^{1}H NMR spectrum of the crude product.

---

* Failing to heat the solution led to much lower yields (~50%)

Presumably the isolated product (**50**) was an equal mixture of both *syn* and *anti* isomers although this could not be verified by NMR analysis. It is expected that both isomers would give almost identical ^{1}H NMR spectra. Although the desired product was not obtained the analysis of the dimer, in conjunction with (**48**), provided further proof of the structure of (**7**) in agreement with results from previous studies.[48] Specifically, the chemical shift of H_a was essentially unaltered upon formation of both (**48**) and (**50**) whereas it would be significantly shifted upfield as a result of expected shielding effects of the nearby aromatic rings if (**7**) had the alternative 'bent' *exo*-adduct structure shown in red in Figure 2.16.

2.4.3 SYNTHESIS OF 5,10,15,20-*TETRAKIS*-(3,5-DI-*TERT*-BUTYLPHENYL)-PORPHYRIN BLOCK (**39**) (^{t}BuPBlock)

2,3-dioxo-5,10,15,20-*tetrakis*-(3,5-di-*tert*-butylphenyl)porphyrin was prepared in 8 steps according to literature methods.[32,46] Key intermediates were analysed using NMR and UV-Vis spectroscopy. The main difference in the preparation of MePBlock (**48**), compared to ^{t}BuPBlock (**39**), was solubility. The 3,5-di-*tert*-butylphenyl porphyrins are generally much more soluble in chlorinated solvents than the analogous 3,5-dimethylphenyl porphyrins and gave much higher yields of the PBlock from the respective porphyrin dione (Scheme 2.11). The ^{1}H NMR spectrum obtained for (**39**) was in agreement with the literature and was directly analogous to that obtained for (**48**).[38] All ^{1}H NMR assignments were, nevertheless, made independently using 2D COSY, 2D NOESY and CH correlated NMR spectral data.

2.5 SYNTHESIS OF PORPHYRIN-SPACER-PORPHYRINS (PSPs)

2.5.1 ACE COUPLING REACTIONS

In terms of the building block assembly approach, toward large rigid spacer groups, the ACE reaction has proven to be a valuable coupling method (Sections 1.4.1 and 1.4.2). The ACE reaction is a [3+2]* cycloaddition between an **A**lkene and a **C**yclobutane **E**poxide. A cyclic 1,3-dipole is formed *in situ* from the ring opening of the cyclobutane epoxide at raised temperatures

---

* Electronically the reaction is classified as a $[_{\pi}4_s + {}_{\pi}2_s]$ cycloaddition between a dipolarophile (alkene 2π component) and a 1,3-dipole (4π component).

(140-160°C) and this undergoes a cycloaddition reaction with a suitably activated alkene, in this case a norbornene moiety (Figure 2.17).[5,50] A key feature, noticed in early studies, was the high *exo,exo*-stereoselectivity when a norbornene dipolarophile was used. The ACE coupling reaction had been used successfully for the formation of analogous systems to those targeted in this work and was, therefore, expected to give similar results using the aryl imide *bis*-epoxide blocks and porphyrin building blocks described in the previous sections and exemplified in Scheme 2.11.

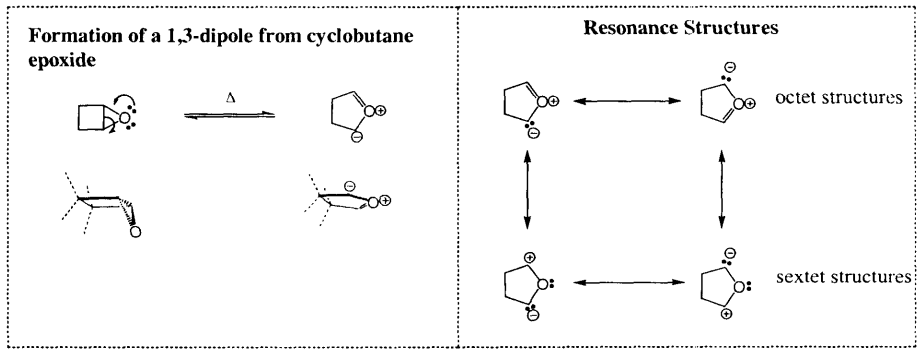

Figure 2.17 Thermal ring-opening of cyclobutane epoxides and formation of a planar pentacyclic 1,3-dipole and contributing resonance structures. These systems are more formally described as 'carbonyl ylides' and are classified as bent 'allyl type' 1,3-dipoles. The numbering (1,3) comes from their propensity to react with dipolarophiles at these positions and not from the positions of formal charges.

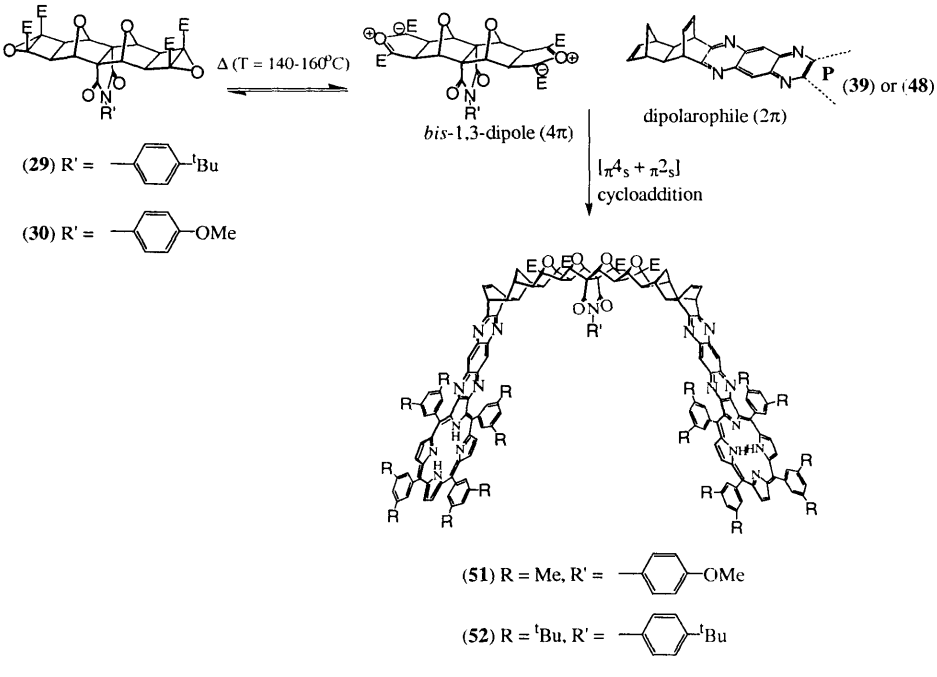

Scheme 2.11 ACE coupling reaction between a centrally functionalised *bis*-cyclobutane epoxide and a porphyrin block.

2.5.2 SYNTHESIS OF PSP (**51**) FROM MePBLOCK (**48**) AND *BIS*-CYCLOBUTANE EPOXIDE (**30**)

For the ACE coupling, MePBlock (**48**) and *bis*-cyclobutane epoxide (**30**) (0.54 equivalents) were heated in a minimum volume of CH_2Cl_2 in a resealable tube at 160°C for a period of 30 hrs. The reaction mixture was monitored by TLC and no significant changes were detected. A repeat of the experiment using half the volume of CH_2Cl_2 had no effect. It was thought that the reduced solubility of MePBlock (**48**) in CH_2Cl_2, compared to ^{t}BuPBlock (**39**), might have been a factor in these failures so a number of other solvent systems were tested, including THF, $CHCl_3$, $CHCl_3$/acetonitrile (3:1), DMF and 1,2-dichloroethane (1,2-DCE). In all these experiments the solvents were carefully purified according to literature methods, in order to exclude moisture and other contaminants. All these reaction mixtures were degassed by freeze thawing before the reaction flasks were flame-sealed under vacuum. Each tube was heated in an oven at 150-160°C for a minimum of 3 days. 1,2-DCE was the only solvent in which the formation of the targeted PSP (**51**) was detected and in this case the yield (< 5%) was disappointingly low. Later experiments showed that yields were not improved with longer reaction times (up to 8 days). It was also found that about 75% of the PBlock (**48**) was recoverable from the reaction mixture after 3 days but the *bis*-epoxide (**29**) could not be detected either by TLC or ^{1}H NMR spectroscopy. The inability to recover the *bis*-epoxide intact after each experiment severely limited both the number of experiments that could be done on varying reaction conditions and also the amount of (**51**) eventually obtained using this method. Nevertheless the small amount of crude product (**51**) obtained was partially purified by flash column chromatography. The product (**51**) was found to have a lower R_f value in all the chlorinated solvent systems used compared to the MePBlock (**48**) starting material and was easily separated from it chromatographically. Subsequent recrystallisations from $CHCl_3$/MeOH gave (**51**) as a fine dark brown solid. Initial analysis of (**51**) was carried out using NMR spectroscopy. The NMR spectrum was generally consistent with the proposed structure (Figure 2.18), however, a number of peaks were present which could not be assigned to the product. The identity of the impurity(s) was not established although it is possible that a small amount of mono-adduct was present as evidenced by similar chemical shifts to the product. Further attempts to purify the PSP (**51**) by recrystallisation proved unsuccessful mainly due to the small amount of product obtained.

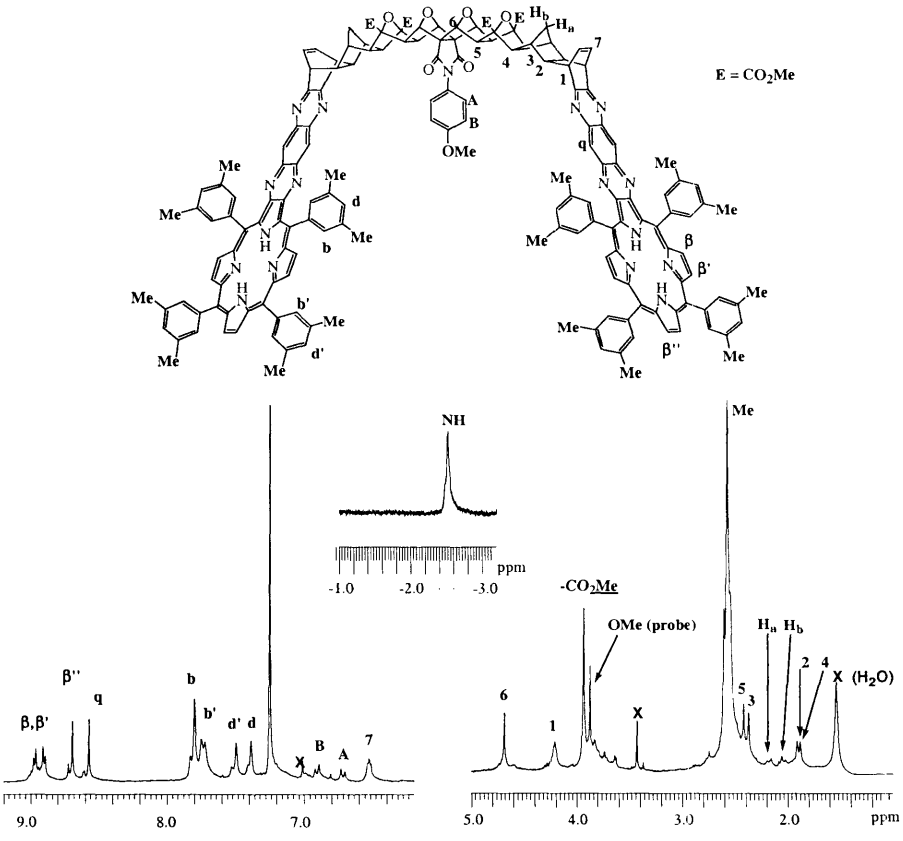

Figure 2.18 ^{1}H NMR of (**51**) (1.5 mg in $CDCl_3$). These tentative assignments were based on 2D COSY results as well as the ^{1}H NMR spectrum of (**52**) below. A small amount of unknown (possibly mono-adduct) porphyrinic impurity was detectable in this sample (e.g. see β" peak) even after chromatographic separation and repeated recrystallisation of the product.

The limited success of the reaction under these standard conditions prompted a detailed investigation of the mechanistic aspects of the reaction, in an effort to rationalise alternative reaction conditions that might be more successful. Historically, arguments about the mechanism of 1,3-dipolar [3+2] cycloaddition reactions have been lively and at times controversial. An amusing personal account by Houk of the developments of pericyclic reaction theory over the last three decades described the famous debates started in the 1960's between Firestone, who proposed a stepwise diradical mechanism, and Huisgen, a strong advocate of a concerted mechanism.[51-57] It is now generally accepted that these reactions normally follow a concerted mechanism* similar to the well-known Diels-Alder reaction mechanism and evidence for this includes the stereospecific retention of configuration in the dipolarophile and insensitivity to solvent polarity.[60] Results from

* Exceptional stepwise 1,3-dipolar cycloadditions have been reported. e.g. (58) Huisgen, R.; Mloston, G.; Langhals, E. *J. Amer. Chem. Soc.* **1986**, *108*, 6401. (59) Huisgen, R.; Mloston, G.; Langhals, E. *J. Org. Chem.* **1986**, *51*, 4085.

high-level quantum mechanical calculations of the transition states of various 1,3-dipolar cycloadditions, including important electron correlation terms, lend further support to the concerted mechanism.[61,62] The rate enhancement of a large number of Diels-Alder cycloadditions by pressure has been well documented and understood in terms of shrinking molecular volumes during the course of reaction. A recent review on this topic lists only a few reactions where activation volumes have been measured for 1,3-dipolar cycloadditions, being in the range of $\Delta V^{\ddagger}$ = -(21 ± 3) cm^3 mol^{-1} indicating that high-pressure conditions may lead to a reaction rate enhancement. The activation volumes, however, are somewhat less (5-10 cm^3 mol^{-1}) than those measured for the related Diels-Alder reactions. Varying results were reported depending on the nature of the 1,3-dipole and dipolarophile involved.[18] As there was a possibility that high-pressure conditions may favour the 1,3-dipolar [3+2] cycloaddition being attempted in this work (ACE reaction), and in light of the dramatic failure of previous attempts to synthesise the target PSP (**51**) using conventional methods, a reaction using high-pressure conditions was carried out. However, no trace of product was detected (TLC or ^{1}H NMR) after the reactants (MePBlock **48** and *bis*-epoxide **30**) were partially dissolved in a small volume of 1,2-dichloroethane (~0.5 mL) and heated at 130°C under a pressure of 10 kbar for 3 days. The maximum temperature that could be used was set by equipment limits and was 10°C less than the temperature range usually used for this reaction (140 - 160°C). Due to dwindling quantities of starting material available further experiments on the ACE reaction under these conditions were not performed and the precise reasons for this last failure remains uncertain. The reaction conditions of all synthetic attempts are summarised in Table 2.5.

It was decided, in light of the significant effort required to make the respective building blocks, that it would be wasteful of both materials and time to repeat the synthesis of (**51**) *in toto*. The alternative tBuPBlock (**39**), proven effective by other workers, was in hand and so it was used in subsequent PSP syntheses. The alternative *bis*-epoxide block (**29**) had also been prepared (Section 2.3) and it was expected that the 'probe' NMR signal for this sub-unit would be larger and, hopefully, less obscured than that found for the OMe group in PSP (**51**) (Figure 2.18).

Table 2.5 Various reaction conditions tested for the synthesis of PSP (**51**).

[MePBlock] (**48**) (mol/L)	[*bis*-epoxide] (**30**) (mol/L)	Solvent	Temperature (°C)	Reaction Time (hrs)	% Yield
0.028	0.015	CH_2Cl_2	160	41	0
0.057	0.030	CH_2Cl_2	160	30	0
0.028	0.015	THF	160	30	0
0.024	0.013	$CHCl_3$	160	72	0
0.028	0.013	$CHCl_3$/MeCN (3:1)	160	72	0
0.012	0.065	DMF	140	49	0
0.021	0.011	1,2-DCE	130 (10 kbar)	72	0
0.028	0.015	1,2-DCE	148	75	<5
0.028	0.015	1,2-DCE	160	192	<5

2.5.3 SYNTHESIS OF PSP (**52**) FROM ^{t}BuPBLOCK (**39**) AND *BIS*-CYCLOBUTANE EPOXIDE (**29**)

^{t}BuPBlock (**39**) and *bis*-epoxide (**29**) (0.54 equivalents) were heated in a minimum volume of CH_2Cl_2 ([^{t}BuPBlock] = 0.021M) in a flame-sealed tube at 150°C for a period of 3 days, resulting in a 53% conversion into the desired PSP (**52**) (Scheme 2.11). The greater solubility of ^{t}BuPBlock (**39**) in the small volumes of solvent (~1 mL) typically used, compared to MePBlock (**48**), was immediately evident and this seems to be an important factor in the difference in yields of the PSPs (**51** and **52**) obtained (see below). It should be noted, however, that significant differences in reactivity between the 5,10,15,20-*tetrakis*-(3,5-dimethylphenyl)-porphyrins and the analogous 5,10,15,20-*tetrakis*-(3,5-di-*tert*-butylphenyl)-porphyrins were noticed in the multi-step synthesis of the respective PBlocks where solubility was not an issue. Most notable were the differences in yields of the quinoxalino-diamine adducts obtained (**38** and **47**) from the respective porphyrin α-

diones (**37** and **46**) (Scheme 2.11), which suggests effects other than solubility may also be responsible for differences in reactivity.

The synthesis was repeated several times and conditions were varied slightly (Table 2.6). The reaction proceeds equally well in dry THF as in CH_2Cl_2 and no improvement in yield was gained by increasing the reaction time. As a significant amount of unreacted ^{t}BuPBlock (**39**) was recovered from each reaction mixture (~30-40%) it was decided to increase the concentration of reactants ([^{t}BuPBlock] = 0.060M) and use a slight excess of the *bis*-epoxide block (**29**) (0.74 equivalents) under the same conditions of temperature and reaction time; however, the yield remained unchanged.

Table 2.6 Various reaction conditions tested for the synthesis of PSP (**52**).

[^{t}BuPBlock] (**39**) ($molL^{-1}$)	[*bis*-epoxide] (**29**) ($molL^{-1}$)	Solvent	Temperature (°C)	Reaction Time (hrs)	% Yield
0.021	0.011	CH_2Cl_2	160	76	53
0.026	0.014	CH_2Cl_2	150	120	30
0.026	0.013	CH_2Cl_2	140	90	40*
0.060	0.044	CH_2Cl_2	150	72	30
0.026	0.014	THF	150	120	30

The scale of these syntheses was relatively small (~25 mg PBlock) and efficient stirring of the reaction mixtures was not possible because of the small diameter of the reaction tubes. To increase the efficiency of the preparation, the synthesis was scaled up by a factor of about three. A new type of reaction flask was designed which allowed for the introduction of a small magnetic stirrer bar to at least maintain, if not improve, the yields from the smaller scale reactions. An added practical bonus was the ease with which materials could be transferred to and from the flask compared with the small narrow reaction tubes previously used. The larger scale reaction was relatively successful giving a yield of 40% of PSP (**52**) (52 mg) after purification by flash column chromatography followed by recrystallisation from CH_2Cl_2/MeOH. The product was analysed by ^{1}H and ^{13}C NMR spectroscopy and all ^{1}H peaks were satisfactorily assigned with the aid of 2D

* larger scale by a factor of ~3.

COSY and 2D ROESY* NMR techniques (Figure 2.19). The assignments were further supported by CH correlated NMR spectra.

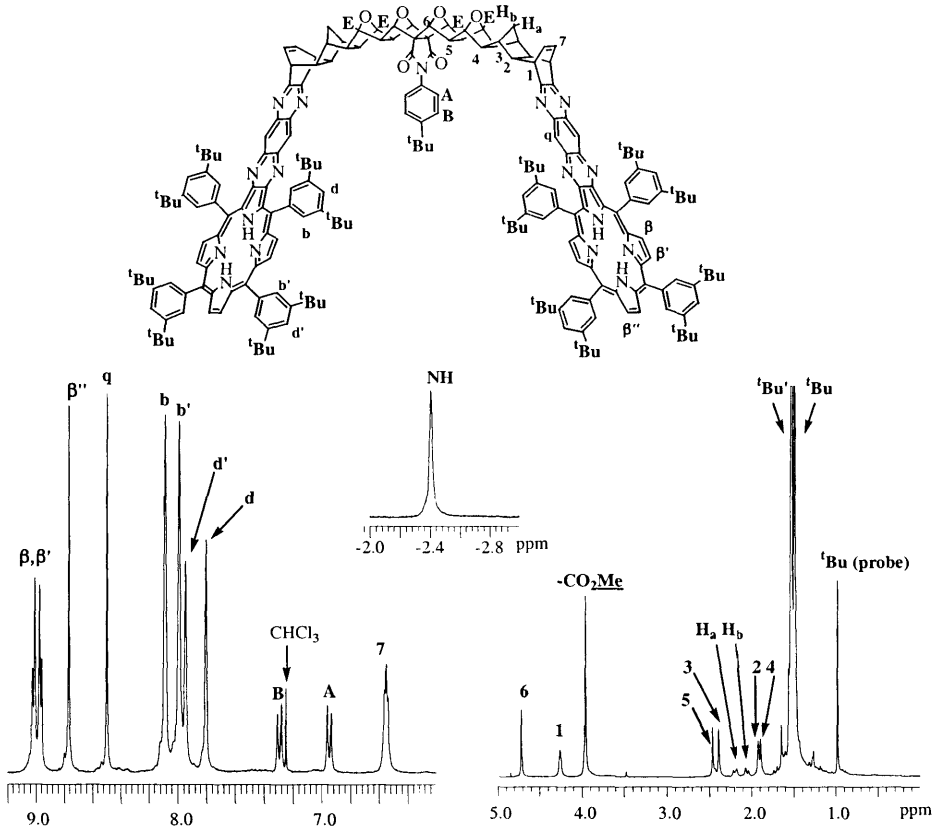

Figure 2.19 ^{1}H NMR spectrum of (**52**). Peak assignments were based on 2D COSY and 2D ROESY spectra as well as CH correlations.

2.6 SUMMARY OF SYNTHESES

A number of *bis*-oxabridged spacer dual blocks have been designed and synthesised in generally moderate yields. These can be coupled to complementary building blocks using well-established procedures either by [2+2] or [4+2] cycloadditions of the *bis*-cyclobutene diesters or ACE coupling of the *bis*-cyclobutane epoxides. The synthesis of centrally functionalised aromatic imides was achieved using room temperature conditions thus avoiding detrimental retro-DA degradation reactions. Introduction of functionality in close proximity to potential bound

* 2D ROESY gave stronger correlations than 2D NOESY. This has been attributed to the size of the molecule and the related tumbling rate through solution. (63) Sanders, J. K. M.; Hunter, B. K. *Modern NMR Spectroscopy - A Guide for Chemists.*; 2nd ed.; Oxford University Press: Oxford, 1993.

substrates is now possible and further development by way of introducing new functional groups will be facilitated by a building block synthetic method adopted.

A new porphyrin block (**48**) was synthesised and its reactivity compared with an analogous porphyrin block (**39**). A stark difference between their propensities to couple to *bis*-epoxides via the ACE reaction was revealed. Although the apparent lower solubility of MePBlock (**48**) is a likely contributing factor it appears that this is not the only reason for its lack of reactivity, as a significant amount of (**48**) was dissolved in the ACE reaction mixtures at the high temperatures used (140-160°C). Although the usefulness of this building block (**48**) in ACE coupling reactions has been shown to be severely limited, other coupling methods may be investigated and hopefully this compound will prove to be useful in future research. The variation of the porphyrin units is important in modulating the behaviour of these systems and one way of achieving this is by changing the peripheral groups on the porphyrin ring. The results from this work suggest that this may not be as straightforward as originally expected.

Two Porphyrin-Spacer-Porphyrins (**51** and **52**) have been synthesised based on each of the two porphyrin blocks described, although (**51**) was obtained in much lower yield than (**52**) and detailed analysis of this compound was therefore limited. Compound (**51**) did prove useful in the initial stages of structural analysis and comparisons were made with results gained from analysis of the analogous PSP (**52**). A detailed structural analysis of (**52**) using a number of different binding studies is described in the following chapter.

Relevant ^{1}H and ^{13}C NMR spectra of key compounds described in Chapter 2 are presented in Appendix A.

References, p. 106

(1) Warrener, R. N.; Abbenante, G.; Kennard, C. H. L. *J. Amer. Chem. Soc.* **1994**, *116*, 3645.

(2) Warrener, R. N.; Abbenante, G.; Solomon, R. G.; Russell, R. A. *Tetrahedron Lett.* **1994**, *35*, 7639.

(3) Warrener, R. N.; Wang, S.; Russell, R. A. *Tetrahedron* **1997**, *53*, 3975.

(4) Warrener, R. N.; Wang, S.; Butler, D. N.; Russell, R. A. *Synlett* **1997**, 44.

(5) Warrener, R. N.; Schultz, A. C.; Butler, D. N.; Wang, S.; Mahadevan, I. B.; Russell, R. A. *Chem. Commun.* **1997**, 1023.

(6) Kallos, J.; Deslongchamps, P. *Can. J. Chem.* **1966**, *44*, 1239.

(7) Maier, G.; Jung, W. A. *Tetrahedron Lett.* **1980**, *21*, 3875.

(8) Warrener, R. N. *Eur. J. Org. Chem.* **2000**, 3363.

(9) Isaacs, N. S. *Liquid Phase HIGH PRESSURE Chemistry*; John Wiley and Sons Ltd.: Brisbane, 1981.

(10) Isaacs, N. S.; George, A. V. *Chem. Brit.* **1987**, *23*, 47.

(11) *High Pressure Chemical Synthesis*; Jurczak, J.; Baranowski, B., Eds.; Elsevier: Amsterdam, **1989**.

(12) Hamann, S. D. *Physico-Chemical Effects of Pressure*; Butterworths Publications Limited: London, 1957.

(13) Amabilino, D. B.; Ashton, P. R.; Balzani, V.; Boyd, S. E.; Credi, A.; Lee, Y.; Menzer, S.; Stoddart, J. F.; Venturi, M.; Williams, D. J. *J. Amer. Chem. Soc.* **1998**, *120*, 4295.

(14) Ballardini, R.; Balzani, V.; Dehaen, W.; Dell'Erba, A. E.; Raymo, F. M.; Stoddart, J. F.; Venturi, M. *Eur. J. Org. Chem.* **2000**, 591.

(15) Acheson, R. M.; Matsumoto, K. *Organic Synthesis at High Pressures*; John Wiley and Sons, Inc.: Toronto, 1991.

(16) van Eldik, R.; Hubbard, C. D. *Chemistry under Extreme and Non-Classical Conditions*; John Wiley and Sons, Inc.: New York, 1997.

(17) Ciobanu, M.; Matsumoto, K. *Liebigs Ann. Chem.* **1997**, 623.

(18) Klarner, F.; Wurche, F. *J. Prakt. Chem.* **2000**, *342*, 609.

(19) Napper, A. M.; Head, N. J.; Oliver, A. M.; Shephard, M. J.; Paddon-Row, M. N.; Read, I.; Waldeck, D. H. *J. Amer. Chem. Soc.* **2002**, *124*, 10171.

(20) Napper, A. M.; Read, I.; Waldeck, D. H.; Head, N. J.; Oliver, A. M.; Paddon-Row, M. N. *J. Amer. Chem. Soc.* **2000**, *122*, 5220.

(21) Head, N. J.; Oliver, A. M.; Look, K.; Lokan, N. R.; Jones, G. A.; Paddon-Row, M. N. *Angew. Chem. Int. Ed.* **1999**, *38*, 3219.

(22) Maier, G.; Jung, W. A. *Chem. Ber.* **1982**, *115*, 804.

(23) Kemp, W. In *Organic Spectroscopy*; 3rd ed.; The Macmillan Press Ltd: London, 1991, p 158.

(24) Warrener, R. N.; Butler, D. N.; Liao, W. Y.; Pitt, I. G.; Russell, R. A. *Tetrahedron Lett.* **1991**, *32*, 1889.

(25) Mitsudo, T.; Kokuryo, K.; Shinsugi, T.; Nakagawa, Y.; Watanabe, Y.; Takegami, Y. *J. Org. Chem.* **1979**, *44*, 4492.

(26) Mitsudo, T.; Naruse, H.; Kondo, T.; Ozaki, Y.; Watanabe, Y. *Angew. Chem. Int. Ed.* **1994**, *33*, 580.

(27) Naota, T.; Takaya, H.; Murahashi, S. *Chem. Rev.* **1998**, *98*, 2599.

(28) Huang, D. J.; Rayabarapu, D. K.; Li, L. P.; Sambaiah, T.; Cheng, C. H. *Chem. Eur. J.* **2000**, *6*, 3706.

(29) Chao, K. C.; Rayabarapu, D. K.; Wang, C.-C.; Cheng, C.-H. *J. Org. Chem.* **2001**, *66*, 8804.

(30) Levison, J. J.; Robinson, S. D. *J. Chem. Soc.(A)* **1970**, 2947.

(31) Hill, J. G.; Rossiter, B. E.; Sharpless, K. B. *J. Org. Chem.* **1983**, *48*, 3607.

(32) Crossley, M. J.; King, L. G. *J. Chem. Soc., Chem. Commun.* **1984**, 920.

(33) Crossley, M. J.; Burn, P. L. *J. Chem. Soc., Chem. Commun.* **1987**, 39.

(34) Crossley, M. J.; Burn, P. L.; Chew, S. S.; Cuttance, F. B.; Newsom, I. A. *J. Chem. Soc., Chem. Commun.* **1991**, 1564.

(35) Crossley, M. J.; Burn, P. L.; Langford, S. J.; Pyke, S. M.; Stark, A. G. *J. Chem. Soc., Chem. Commun.* **1991**, 1567.

(36) Crossley, M. J.; Burn, P. L. *J. Chem. Soc., Chem. Commun.* **1991**, 1569.

(37) Crossley, M. J.; Burn, P. L.; Langford, S. J.; Prashar, J. K. *J. Chem. Soc., Chem. Commun.* **1995**, 1921.

(38) Warrener, R. N.; Johnston, M. R.; Gunter, M. J. *Synlett* **1998**, 593.

(39) Johnston, M. R.; Gunter, M. J.; Warrener, R. N. *Chem. Commun.* **1998**, *21*, 2739.

(40) Schultz, A. C.; Johnston, M. R.; Warrener, R. N.; Gunter, M. J. Electronic Conference on Heterocyclic Chemistry '98, **1998**.

(41) Warrener, R. N.; Schultz, A. C.; Johnston, M. R.; Gunter, M. J. *J. Org. Chem.* **1999**, *64*, 4218.

(42) Johnston, M. R.; Latter, M. J.; Warrener, R. N. *Aust. J. Chem.* **2001**, *54*, 633.

(43) Johnston, M. R.; Gunter, M. J.; Warrener, R. N. *Tetrahedron* **2002**, *58*, 3445.

(44) Johnston, M. R.; Latter, M. J.; Warrener, R. N. *Org. Lett.* **2002**, *4*, 2165.

(45) Warrener, R. N.; Suna, H. S.; Johnston, M. R. *Aust. J. Chem.* **2003**, *56*, 269.

(46) Baldwin, J. E.; Crossley, M. J.; DeBernadis, J. *Tetrahedron* **1982**, *38*, 685.

(47) Catalano, M. M.; Crossley, M. J.; Harding, M. M.; King, L. G. *J. Chem. Soc., Chem. Commun.* **1984**, 1535.

(48) Warrener, R. N.; Johnston, M. R.; Schultz, A. C.; Golic, M.; Houghton, M. A.; Gunter, M. J. *Synlett* **1998**, 590.

(49) Snyder, E.; Franzus, B. *J. Amer. Chem. Soc.* **1964**, *86*, 1166.

(50) Warrener, R. N.; Butler, D. N.; Margetic, D.; Pfeffer, F. M.; Russell, R. A. *Tetrahedron Lett.* **2000**, *41*, 4671.

(51) Houk, K. N. *Acc. Chem. Res* **1995**, *28*, 81.

(52) Firestone, R. A. *J. Org. Chem.* **1968**, *33*, 2285.

(53) Firestone, R. A. *J. Org. Chem.* **1972**, *37*, 2181.

(54) Firestone, R. A. *J. Org. Chem.* **1976**, *41*, 2212.

(55) Huisgen, R. *Angew. Chem. Int. Ed.* **1963**, *2*, 633.

(56) Huisgen, R. *J. Org. Chem.* **1968**, *33*, 2291.

(57) Huisgen, R. *J. Org. Chem.* **1976**, *41*, 403.

(58) Huisgen, R.; Mloston, G.; Langhals, E. *J. Amer. Chem. Soc.* **1986**, *108*, 6401.

(59) Huisgen, R.; Mloston, G.; Langhals, E. *J. Org. Chem.* **1986**, *51*, 4085.

(60) *1,3-Dipolar Cycloaddition Chemistry*; Padwa, A., Ed.; Wiley Interscience: New York, **1984**; Vol. 1-2.

(61) Rastelli, A.; Gandolfi, R.; Amade, M. S. *J. Org. Chem.* **1998**, *63*, 7425.

(62) Valentin, C. D.; Freccero, M.; Gandolfi, R.; Rastelli, A. *J. Org. Chem.* **2000**, *65*, 6112.

(63) Sanders, J. K. M.; Hunter, B. K. *Modern NMR Spectroscopy - A Guide for Chemists.*; 2nd ed.; Oxford University Press: Oxford, 1993.